Analysis of the Mechanisms of Factor XII Activation

M.Sc. Laura Heikaus

Dissertation

for the acquisition of the academic degree

Dr. rer. nat.

at the

University of Hamburg

Faculty of Mathematics, Informatics and Natural

Sciences Department of Chemistry

and the

University Medical Center Hamburg-Eppendorf

Institute for Clinical Chemistry and Laboratory Medicine

Mass Spectrometric Proteomics Group

June 2019

Disputation und Druckfreigabe am 27.09.2019

Reviewers

Prof. Dr. Hartmut Schlüter

Prof. Dr. Sascha Rohn

Research for this thesis was carried out in the Mass Spectrometric Proteomics Group of Prof. Dr. Hartmut Schlüter at the University Medical Center Hamburg-Eppendorf from August 2015 until June 2019.

List of publications

1.   Fazel, Ramin; Guan, Yudong; Vaziri, Behrouz; Krisp, Christoph; **Heikaus, Laura**; Saadati, Amirhossein; Nurul Hidayah, Siti; Gaikwad, Manasi; Schlüter, Hartmut. **/** Structural and In Vitro Functional Comparability Analysis of Altebrel™, a Proposed Etanercept Biosimilar: Focus on Primary Sequence and Glycosylation. in: Pharmaceuticals (Basel, Switzerland). 2019; Jahrgang 12, Nr. 1.

2.   Hänel, Lorena; Kwiatkowski, Marcel; **Heikaus, Laura**; Schlüter, Hartmut. / Mass spectrometry-based intraoperative tumor diagnostics. in: Future Science OA. 2019.

3.   Hänel, Lorena; Gosau, Tobias; Maar, Hanna; Valentiner, Ursula; Schumacher, Udo; Riecken, Kristoffer; Windhorst, Sabin; Hansen, Nils-Owe; **Heikaus, Laura**; Wurlitzer, Marcus; Nolte, Ingo; Schlüter, Hartmut; Lange, Tobias. / Differential Proteome Analysis of Human Neuroblastoma Xenograft Primary Tumors and Matched Spontaneous Distant Metastases. in: SCI REP-UK. 2018; Jahrgang 8, Nr. 1. S. 13986.

4.   Weidmann, Henri; **Heikaus, Laura**; Long, Andy T; Naudin, Clément; Schlüter, Hartmut; Renné, Thomas. / The plasma contact system, a protease cascade at the nexus of inflammation, coagulation and immunity. in: BBA-MOL CELL RES. 2017; Jahrgang 1864, Nr. 11 Pt B. S. 2118-2127.

5.   Kornecki, Martin; Mestmäcker, Fabian; Zobel-Roos, Steffen; **Heikaus, Laura**; Schlüter, Hartmut; Strube, Jochen. / Host Cell Proteins in Biologics Manufacturing: The Good, the Bad, and the Ugly. in: ANTIBODIES. 2017; Jahrgang 6, Nr. 3. S. 13.

6.   Fuh, Marceline Manka; **Heikaus, Laura;** Schlüter, Hartmut. / MALDI mass spectrometry in medical research and diagnostic routine laboratories. in: INT J MASS SPECTROM. 2017; Jahrgang 416, Nr. Special Issue. S. 96-109.

Table of contents

Protein nomenclature, abbreviations and conventions

1. The single letter amino acid code is used (table 1).

2. Within this thesis the amino acid positions are used according to the Uniprot database. Meaning that residue 1 is the starting methionine (M).

3. The protein names and corresponding abbreviations used are specified in table 1 as well as the corresponding unique Uniprot accession number.

Table 1: Single letter amino acid code

G	Glycine	P	Proline
A	Alanine	V	Valine
L	Leucine	I	Isoleucine
M	Methionine	C	Cysteine
F	Phenylalanine	Y	Tyrosine
W	Tryptophan	H	Histidine
K	Lysine	R	Arginine
Q	Glutamine	N	Asparagine
E	Glutamic Acid	D	Aspartic Acid
S	Serine	T	Threonine

Table 2: List of Proteins with corresponding abbreviations used in this work.

UniProt ID	Protein name (Used in thesis)	Abbreviation	Gene	Synonyms found in literature
P00748	Factor XII (Active FXII)	FXII (FXII a)	F12	Coagulation Factor XII Hageman factor
P03952	Plasma (pre-) kallikrein	PK (PPK)	KLKB1	Fletcher factor Kininogenin
P01042	High molecular weight kininogen	HK	KNG1	Fitzgerald factor -
	Low molecular weight Kininogen	LK	KNG1	-
	Bradykinin	BK	KNG1	Kallidin I
P01008	Antithrombin III	ATIII	SERPINC1	Serpin C1
Q14520	Hyaluronan-binding protein 2	HABP2	HABP2	Factor seven-activating protease (FSAP)
P01023	Alpha-2-Macroglobulin	α2M	A2M	-
P00747	Plasmin (Plasminogen)	-	PLG	Zymogen: Plasminogen Active form: Plasmin.
P02671 P02675 P02679	Fibrin (Fibrinogen (α, β, γ))	-	FGA FGB FGG	Zymogen: Fibrinogen α, β and γ Insoluble polymer: Fibrin
Q12884	Antiplasmin-cleaving enzyme	APCE	FAP	Fibroblast activation protein alpha
P08697	Alpha-2-antiplasmin	α2AP	SERPINF2	Alpha-2-plasmin inhibitor Serpin F2
P05155	C1 esterase inhibitor	C1-inh	SERPING1	Serpin G1

Table 3: Abbreviations used in this work.

Term	Abbreviation
Acetonitrile	ACN
chain ejection model	CEM
charge residue model	CRM
Dextran sulfate	DXS
Dithiothreitol	DTT
Electrospray ionization	ESI
evaporation model	IEM
Formic acid	FA
Hereditary angioedema	HAE
Iodoacetamide	IAA
Liquid chromatography	LC
Mass spectrometry	MS
Matrix assisted laser desorption ionization	MALDI
Phosphate buffer saline	PBS
polyacrylamide gel electrophoresis	PAGE
Polyphosphate	PolyP
Reversed-phase	RP
Sodium dodecyl sulfate	SDS
Ultra-High-Performance liquid chromatography	UHPLC

Zusammenfassung

Die Kontaktsystemaktivierung erfolgt durch das Binden des Faktor XII (FXII)-Zymogens an negativ geladene Oberflächen. Die aktivierte FXII-Spezies löst eine proteolytische Kaskade aus. Die ablaufenden proteolytischen Prozesse führen zur Spaltung von hochmolekularem Kininogen (HK) und in der Folge zur Freisetzung des Peptidhormons Bradykinin (BK). BK wiederrum löst eine Entzündungsreaktion aus. Zusätzlich zur Entzündungsreaktion aktiviert FXII auch die intrinsische Gerinnungskaskade. Interessanterweise zeigen FXII-defiziente Individuen keinerlei Gerinnungsstörungen. Diese Besonderheit macht FXII zu einem interessanten Ziel für antithrombotische Wirkstoffe. In Studien zur FXII-Aktivierung wurde gezeigt, dass FXII durch Polyphosphat (PolyP) und Dextransulphat (DXS) aktiviert wird und nachfolgende Entzündungsprozesse eingeschaltet werden. Durch PolyP aktiviertes FXII führt zusätzlich zur Aktivierung der intrinsischen Gerinnung.

Ziel dieser Arbeit war es, die molekularen Mechanismen der FXII-Aktivierung durch PolyP und DXS zu identifizieren. Zur Beantwortung dieser Frage wurde ein sogenannter Migrationsprofil-Assay genutzt. Dieser Ansatz erlaubte es, die durch Proteolyse entstanden unterschiedlichen Proteinspezies aus einem komplexen Proteingemisch zu identifizieren. Mittels der Migrationsprofile lassen sich auch Fusionsproteine bestehend aus Protease und Inhibitor, wie zum Beispiel der FXII–C1-Inhibitor-Komplex, identifizieren.

Die PolyP-vermittelte FXII-Aktivierung resultierte in einer aktiven FXII-Spezies in voller Länge. Hingegen führte die DXS-vermittelte FXII-Aktivierung zu einer aktiven proteolytisch gespaltenen FXII-Spezies. In beiden Fällen wurde durch proteolytische HK-Spaltung die Entzündungsreaktion induziert. Darüber hinaus konnte gezeigt werden, dass in Gegenwart von DXS der Serin-Protease-Inhibitor Antithrombin III aktiviert wird. Die Aktivierung des FXII durch PolyP hat die proteolytische Aktivierung des Hyaluronan-bindenden Protein 2 (HABP2) zur Folge. Aus diesen Ergebnissen kann die Schlussfolgerung gezogen werden, dass *in vivo* DXS-ähnliche Moleküle die

Gerinnung über Faktor XI inhibieren und PolyP die Faktor-VII-vermittelte Gerinnung unterstützt.

FXII-Aktivierung hat auch eine proteolytische Spaltung von Inter-alpha-trypsin inhibitor heavy chain 4 (ITIH4) zur Folge. Die proteolytisch gespaltene ITIH4-Spezies kann an Bikunin binden, sodass Bikunin seine Proteaseinhibitorfunktion entfalten kann. Dennoch sind die genauen Funktionen und Mechanismen des ITIH4-Bikunin-Komplexes weiterhin unbekannt.

Zusammenfassend konnten die Aktivierungsmechanismen des FXII durch PolyP und DXS anhand der nachgewiesenen unterschiedlichen Proteinspezies erklärt werden. Diese haben eine deutlich unterschiedliche Konformation und Substratspezifität, welche die Gerinnung unterschiedlich beeinflussen.

Abstract

The plasma contact system is a complex proteolytic cascade activated by binding of factor XII (FXII) zymogen to negatively charged surfaces to form active FXII species. Active FXII triggers an inflammatory response by the proteolytic release of bradykinin (BK) from its precursor high molecular weight kininogen (HK) and the intrinsic pathway of coagulation. FXII deficient individuals do not suffer from any bleeding disorder and are, in addition, protected against thrombosis. Therefore, FXII has become an interesting target for the development of anti-thrombotic drugs. Studies of the FXII revealed that coagulation occurs depending on the molecule activating FXII: activation of FXII by Polyphosphate (PolyP) induces coagulation whereas, activation by dextran sulfate (DXS) does not. FXII activated by either molecule induces the bradykinin formation.

The aim of this work was to decipher the molecular mechanisms underlying FXII activation by PolyP and DXS. The plasma proteome was analyzed with mass spectrometry after separation of the intact proteins on an SDS-PAGE. This migration profile assay allows for the identification of different protein species within complex protein mixtures such as plasma, which are formed by proteolytic degradation or formation of fusion proteins by e.g. covalent binding of proteases to their inhibitors.

FXII activation by PolyP results in a full-length active FXII-species whereas activation with DXS results in a proteolytically cleaved two chain FXII-species. Both species promote HK cleavage and as a result BK release. Moreover, it was shown that in presence of DXS, the serine protease inhibitor antithrombin III is activated. The activation of FXII by PolyP results in the proteolytically activated hyaluronan binding protein 2 (HABP2). From these results it can be concluded that in vivo DXS-like molecules inhibit the coagulation cascade via factor XI (FXI) and PolyP enhances coagulation via factor VII (FVII).

Activation of FXII by PolyP results in the proteolytic processing of inter-alpha-trypsin inhibitor heavy chain 4 (ITIH4). The proteolytically cleaved species of ITIH4 is able to

bind to bikunin enhancing its inhibitory activity towards proteases. However, the exact role of the ITIH4-bikunin complex with respect to the contact system remains to be discovered.

In summary, the activation mechanisms of FXII by PolyP and DXS could be explained by identification of the resulting protein species. These FXII species have a different conformation and specificity that influence the coagulation cascade in a different manner.

Introduction

Mass spectrometric proteomics

The term 'proteome' was introduced in 1995[1] in analogy to the term 'genome' and is used to describe the complete set of proteins present in a given organism, tissue or cell type at a given time point. Contrary to the genome, which is constant in all cells of a single organism, the proteome of each cell or tissue is highly variable. The protein composition of a cell depends on its function, state and several environmental influences. After decades of tedious protein research using 2D-Gel electrophoresis encountering many problems, such as lack in reproducibility and difficulty in the identification of the spots, developments in the field of mass spectrometry (MS) revolutionized the field of proteome research[2]. Mainly two main advances contributed to the growing application of MS methods for proteomics: the availability of genome databases and the development of soft ionization methods[3], namely matrix assisted laser desorption ionization (MALDI)[4] and electrospray ionization (ESI)[5]. Even though, substantial progress in the analysis of intact proteins (*top-down* proteomics) has been achieved, the *bottom-up* approach is still considered the method of choice for the identification and quantification of proteins in complex samples. In this technique, the proteins in the mixture are subjected to tryptic digestion and the resulting peptides are analyzed. The identification of peptides and the respective protein they originated from, is aided by database search[6].

Ionization

Mass spectrometry (MS) relies on the detection of charged molecules. Therefore, the molecules are ionized in the source, the mass to charge ratio (m/z) is analyzed in the mass analyzer, to finally produce a signal in the detector.

Although, broadly differing in their mechanism, MALDI and ESI are so called "soft ionization techniques", specially developed for the ionization of biomolecules. MALDI[4] relies on the co-crystallization of the analyte with the acidic matrix molecules. A laser beam, typically in the UV range, excites the aromatic rings of the matrix molecules, propelling them into the gas phase. The co-crystallized biomolecules receive a proton from the acid and are dragged into the gas phase. This technique is a discontinuous ionization method, since the ionization takes place after each laser shot onto the crystallized sample. On the contrary, ESI[5] is a continuous ionization technique, relying on the fine spray of the dissolved sample from a needle (emitter). A voltage is applied to the emitter aiding in the formation of the positively charged droplet spray. Drying gas evaporates the excess solvent and, as the droplets shrink, charge density increases. As a consequence, the repulsion between the charges increases, until the surface tension of the liquid can no longer withstand the pressure and the droplet splits into multiple smaller droplets, also referred to as coulomb explosion[7,8] (figure 1).
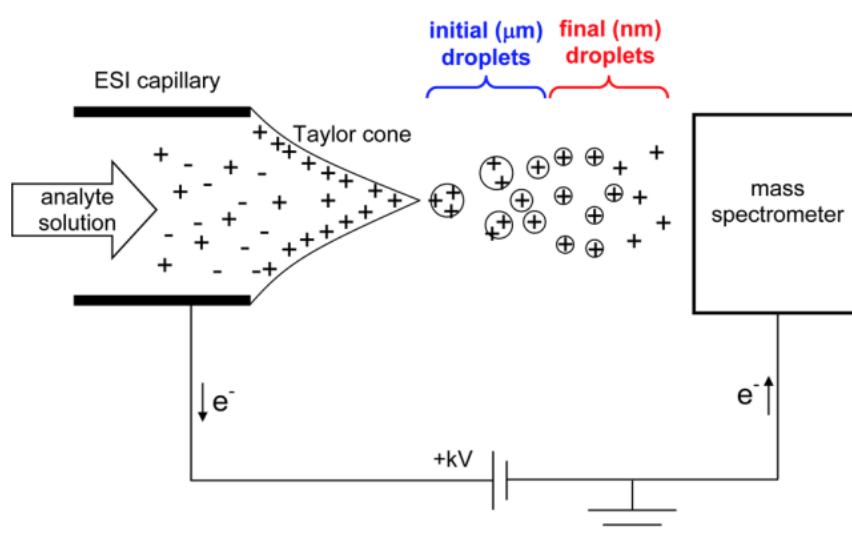

Figure 1: Schematic representation of droplet formation in an electrospray ionization (ESI) source[9].

The ultimate ionization of the analyte can be explained by three models: the ion evaporation model (IEM), the charge residue model (CRM) or the chain ejection model (CEM) (figure 2). While the IEM best describes the ion formation of small molecules, where the charged analyte is directly ejected from the droplet, the CRM is better suited to explain the formation of ions from biomolecules stating that the excess charges from the droplets remain on the analyte molecules after solvent evaporation. The third model, CEM is a more recent approach combining both CRM[10] and IEM[11]. This model best explains the ionization of denaturated proteins. The unfolded proteins are pushed to the surface of the droplet by hydrophobic and electrostatic forces. Subsequently, the protein gradually ejects from the solvent, forming a tail like structure out of the droplet[10].
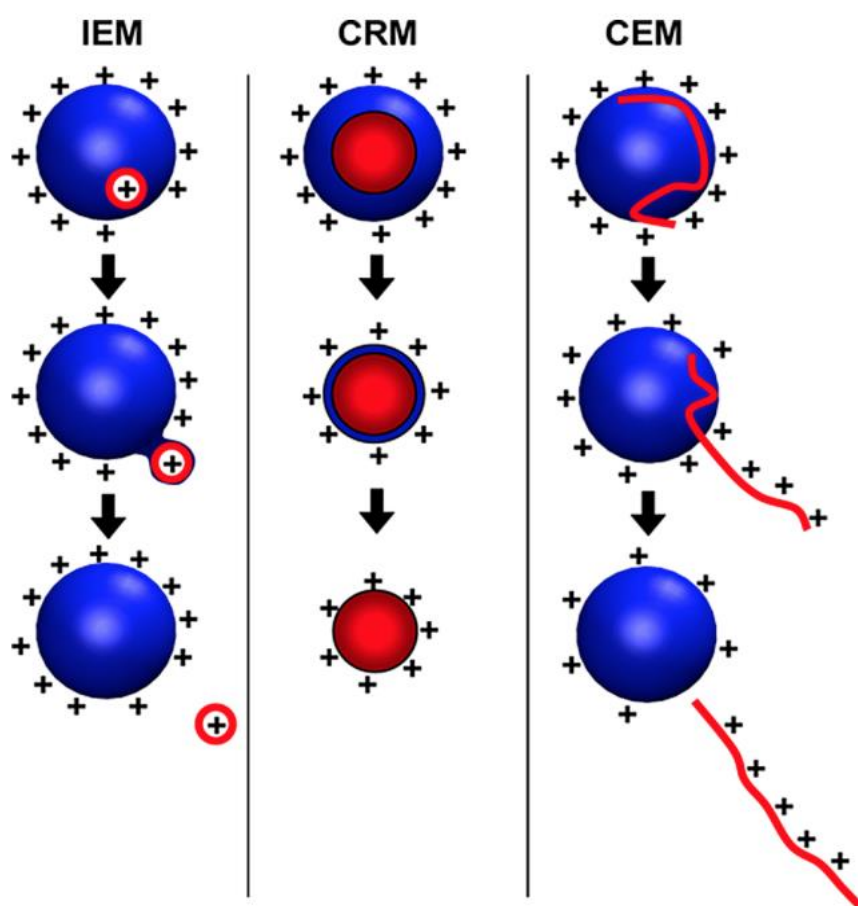

Figure 2: Schematic representation of the three proposed ionization mechanisms. Ion ejection model (IEM), charged residue model (CRM) and chain ejection model (CEM)[9].

Mass analyzers

After ionization, the analytes are guided through a vacuum into the mass analyzer, determining their m/z. Several types of mass analyzers have been developed over the years, differing in the field of application, sensitivity and mass resolution, namely, the quadrupole, ion trap, time of flight, ion cyclotron resonance and most recently the orbitrap. The mass analyzers relevant to this work are the quadrupole, the orbitrap and the ion trap.

Typically, the quadrupole consists of four pairwise parallel rod-shaped electrodes. A voltage is applied to each pair of opposing electrodes and a radio frequency is responsible for alternating the charges of the electrodes. In dependence of the frequency, ions with a specific m/z or within a set m/z window are guided through the quadrupole on a stable flight path. Ions beyond this specific m/z value or window will be filtered out. Hence, this mass analyzer is most commonly used as a continuous mass filter and usually followed by another analyzer for tandem mass spectrometry.

The ion trap is composed of a ring electrode and an endcap electrode. The voltage applied to each electrode is alternated, creating oscillating electric fields. The switching of the voltage is done in a radio frequency time range, faster than it would take the ions to escape the field and therefore, resulting in their entrapment. Specific m/z can be selectively released from the trap adjusting the frequency[12,13]. Both, ion trap and quadrupole require the connection to a detector. Typically, a micro-channel plate detector is used, that multiplies the impact of the ions via secondary emission and converts it into an electric signal.

The orbitrap is one of the most recent developed mass analyzers[14,15]. In analogy to the ion trap, it also traps the ions in an electric field. The electrodes however, are differently organized. One outer barrel-shaped electrode is formed around one inner spindle-shaped electrode to trap the ions in an orbital motion around the inner electrode. The ions enter the orbitrap when the field between the electrodes is reduced. Therefore, and to be in the same phase all ions have to enter the orbitrap at the same time. This

is achieved by creating ion packages in the C-trap – curved linear ion trap. The ions are ejected simultaneously from the C-trap into the orbitrap where the voltage is ramped up to increase the electric field. Apart from the orbital motion, the ions oscillate along the central electrode in dependence on their m/z. The frequency of the oscillation induces an image current at an electrode outside the trap. Using the Fourier transformation, the signal from the electrode is converted into a spectrum. The detection of all ions in the orbitrap at the same time allows to acquire a better signal to noise ratio. The resolution can be increased by increasing the time in which the ions remain in orbit.

In hybrid mass spectrometers such as the orbitrap Fusion, used in this work, different mass analyzers are combined and used in parallel (figure 3). Combining the mass accuracy and resolution provided by the orbitrap, it is used to accurately acquire the spectra of the intact ions (MS1). Simultaneously, the fragment spectra (MS2) are produced and recorded in the ion trap, in order to use one cycle time to acquire as many MS2 spectra as possible for each MS1 and therefore, increasing the number of identified peptides[15].
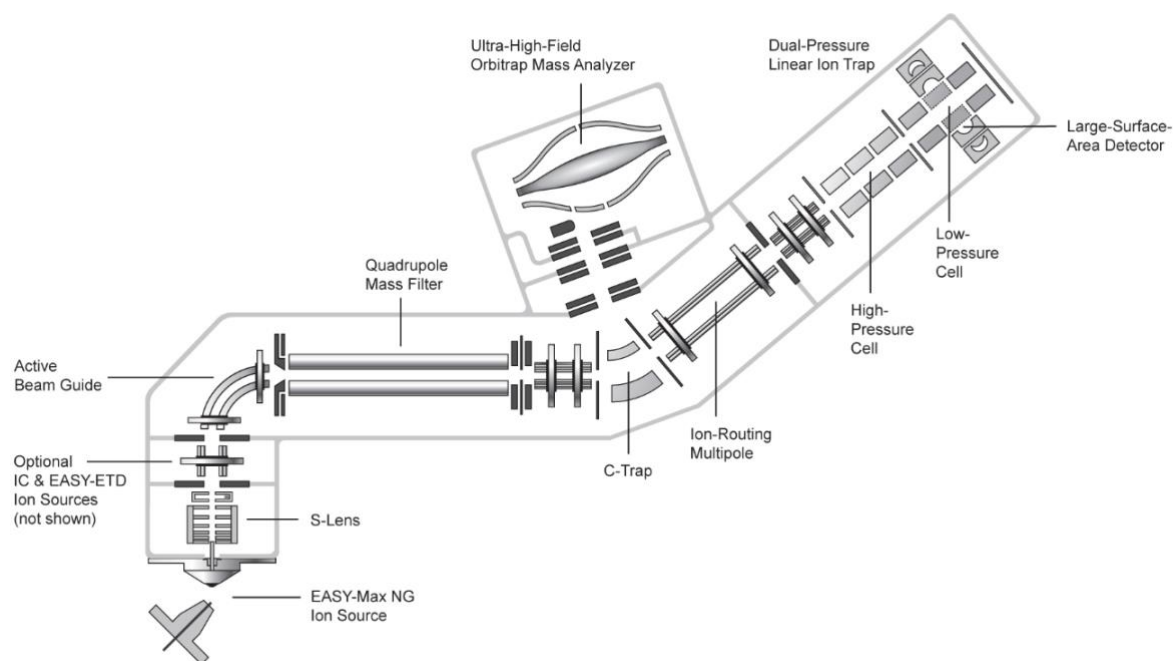
Figure 3: Spatial arrangement of an Orbitrap Fusion mass spectrometer (Thermo Fisher Scientific). The first mass analyzer is a quadrupole used for the selection of the precursor ions. The C-trap collects the ions for acquisition in the orbitrap. The ion routing multipole can direct the ions to and from the ion-trap. The Ion trap can be used as mass analyzer or as collision cell to produce fragment ions that can be guided to the detector or re-routed into the orbitrap for detection (planetorbitrap.com, Thermo Fisher Scientific, 2019)[16].

Peptide fragmentation

Coupling mass analyzers in series (tandem mass spectrometry) provides the ability to select and fragment ions with a specific m/z and analyze their fragments in a fragment spectrum (MS2). This approach is applied in proteomics to acquire sequence information of the analyzed peptides. Therefore, peptide ions analyzed at MS1 level are selected for fragmentation, usually by collision induced dissociation (CID). The selected peptide ion is guided into the collision cell where it is accelerated and collides with an inert gas producing fragments[17]. Fragmentation occurs primarily at the peptide bond, producing fragments with a mass difference of one amino acid. Hence, the MS2 spectra of the peptide containing its sequence information.

Sequence identification

The sequence database driven search is the method of choice for the identification of peptides from fragment spectra in large data sets. The databases are generated from genomic sequencing, containing all possible amino acid sequences of an organism. For a given precursor ion, a list of possible peptides is generated after in silico digestion of the database. Each MS2 spectrum is then matched against the theoretical MS2 spectra of the candidate peptides and a score is calculated. According to the database, the highest scoring peptide is then assigned to their protein of origin[18].

Separation techniques in proteomics

Infusing complex peptide mixtures into a mass spectrometer generates very complex spectra which cannot be fully analyzed even by modern mass spectrometers with high sensitivity and mass accuracy. Factors like ionization probability, ion suppression and the dynamic range of the proteins in a given sample are obstacles to overcome in the identification. In bottom-up proteomics, separating the peptides before they enter the mass spectrometer is a way to reduce these problems. Commonly used is the reversed-phase (RP) liquid chromatography (LC), where peptides are separated according to their hydrophobicity. In this technique, the peptides are loaded onto the stationary phase (column) and bind to it by hydrophobic interactions. Altering the composition of the liquid phase, changing it from an aqueous to a more organic solvent, these interactions are weakened and the peptides elute from the column. The resulting continuous flow of peptides is coupled to a mass spectrometer with an ESI source, allowing for the continuous ionization of the eluting peptides. This set-up is called LC-MS/MS and is the contemporary method of choice in *bottom-up* proteomics[19]. Separating the peptides of each sample before they enter the MS, provides an enormous increase in the identification rate, as well as the sequence coverage (amino acid percentage identified of each protein). Fractionation of a sample prior to LC-MS/MS analysis reduces its complexity. Introducing a second dimension of LC, for example high pH or ion exchange provides a separation on peptide level. On protein

level, the isoelectric focusing (IE) or the sodium dodecyl sulfate polyacrylamide gel electrophoresis (SDS-PAGE) are commonly applied.

SDS-PAGE

The SDS-PAGE is a method used to separate proteins based on their molecular weight. Under reducing conditions, proteins lose their tertiary structure due to denaturation and cleavage of the disulfide bonds. Sodium dodecyl sulfate (SDS) acts as a detergent. With its 12-carbon hydrophobic tail, it interacts with the primary structure of a proteins, whereas the negatively charged sulfate group points outward (figure 4). Therefore, the proteins remain denaturated, in solution and their intrinsic charge is masked, resulting in all proteins in the solution acquiring the same negative mass to charge ratio.
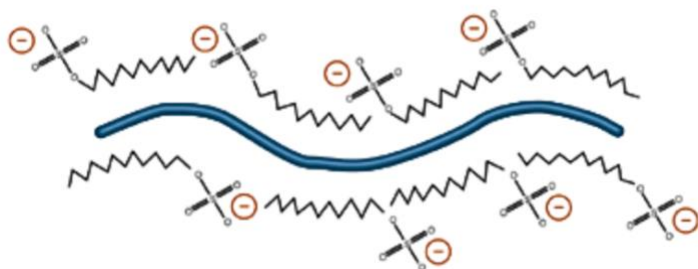

Figure 4: Schematic representation of SDS molecules interacting with the primary structure of the proteins via their hydrophobic C12 tail. (www.nationaldiagnostics.com. 2019)[20]

The protein mixture is applied onto a polyacrylamide gel surrounded by an electrolyte containing buffer. By application of a voltage, the negatively charged proteins move towards the anode. The porous gel offers a resistance to the molecules according to their molecular weight, resulting in their separation. Smaller proteins travel faster through the gel and the larger ones are retained at the top, near the cathode. As a result, the proteins are separated in bands along the gel according to their molecular weight. Staining with silver, Coomassie brilliant blue or other dyes make the bands visible[21,22].

Human plasma proteome

The human plasma is a complex fluid holding a vast amount of lipids, metabolites, ions, peptides and proteins with a concentration of 60 to 80 mg/ml[23]. Proteins are effector molecules with diversified functions, such as transport, storage, signaling and catalysis. Several pathways are regulated by over 1200 known and putative proteases[24,25]. Many proteins circulate as inactive pro-enzymes (zymogens) and are activated upon cleavage. Since many signaling proteins are inactivated by proteolytic degradation, a strict regulation of proteolytic activation and inhibition of proteases is therefore essential. The large abundance and variety of proteases requires a proportional amount of inhibitors. These inhibitors represent about 10 % of the total proteins in the plasma[26] and are able to inhibit proteases by various mechanisms.

Serine proteases

Proteases are enzymes that catalyze the hydrolysis of the peptide bond. They can be classified into six families in accordance to their catalytic residue: serine, threonine, cysteine, asparagine, aspartic and glutamic acid. The seventh protease family is constituted by the metalloproteases that have a metal ion, usually zinc, in the catalytic site. The most relevant proteases to this work belong to the serine protease family. Even though serine proteases vary in their size, sequence and structure, they are all characterized by the highly conserved catalytic triad. The catalytic triad is composed of three amino acids: histidine, aspartic acid and serine. Even though they lie several amino acids apart in the primary structure, the three-dimensional folding of the protease brings them into perfect special arrangement. The serine acts as a neutrophil, the histidine as a base and the aspartate as an acid. The general mechanism of proteolysis is divided into two parts (figure 5)[27]: First acylation takes place. The basic N from the histidine subtracts a proton from the serine. Subsequently, the nucleophilic attack from the serine to the carbonyl of the peptide substrate yields a tetrahedral intermediate and the resulting histidine-H_+ is stabilized by a hydrogen bond to the aspartic acid. The C-terminus of the substrate (leaving group) is expelled when the

histidine-H+ acts as an acid and the tetrahedron collapses, yielding the acylenzyme intermediate.
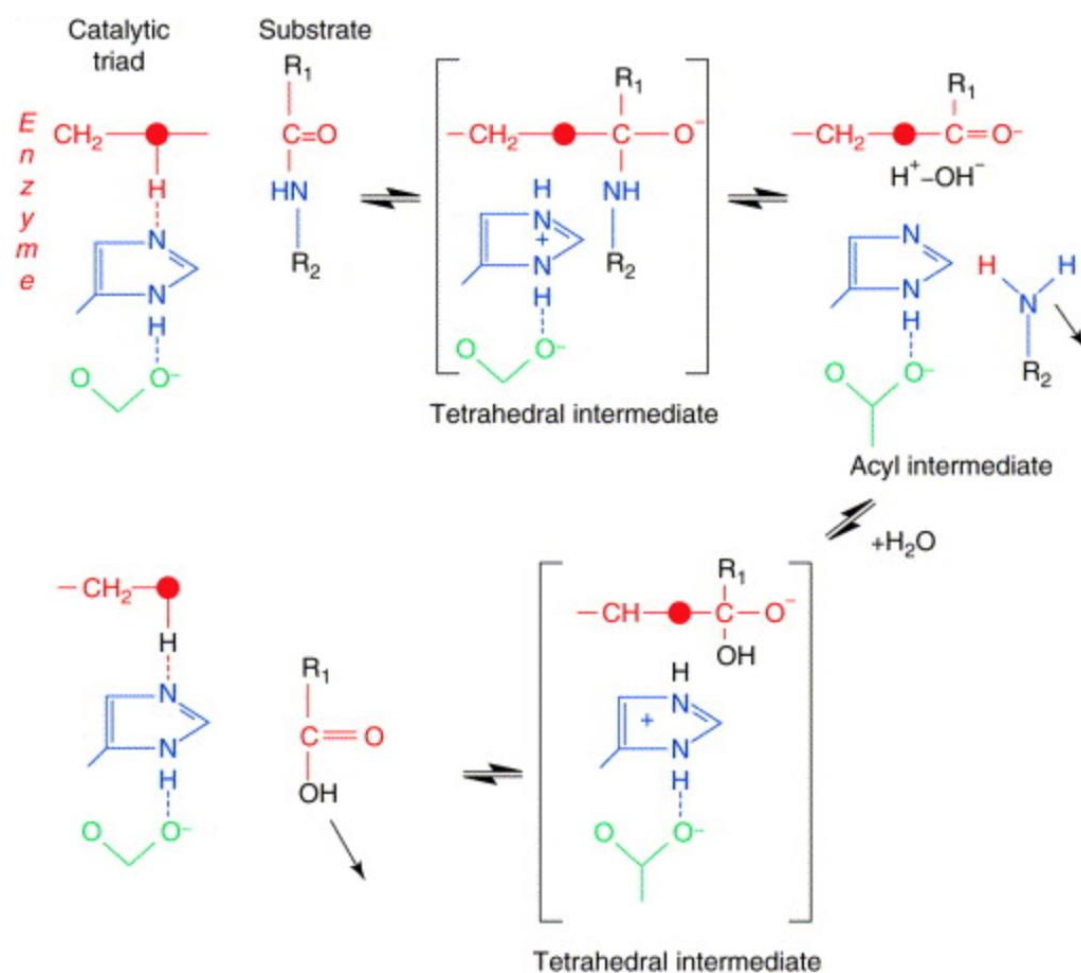

Figure 5: Nucleophilic attack on the peptide bond by the catalytic triad. The nucleophilic residue is shown in red (red dot indicates the nucleophilic atom). The histidine is shown in blue and the acidic residue are in green[27].

In the second part (deacylation) the histidine assists a water attack to the acylenzyme. When this second tetrahedral intermediate collapses the N-terminal cleavage products are released and the catalytic triad regains its initial state. Reviews from Dodson et al. [27] and Hedstrom et al. [28] offer a structural and chemical view on catalytic triads.

Serine protease inhibitors

Serine proteases can be inhibited irreversibly by their specific inhibitors, the serpins. These proteins are usually between 350 and 400 amino acids long and possess a flexible reactive center loop with a cleavable peptide bond. The native structure of serpins is metastable, meaning that their three-dimensional structure is not the most thermodynamically stable form. Cleavage of the reactive peptide bond by the target protease induces a rapid conformational change into the most stable form. The C-terminus of the reactive center loop is masked by the conformational change and can no longer leave the reactive site of the protease and remains covalently bound to the reactive serine. A protease-serpin complex is irreversibly formed, serpins are thus suicide inhibitors.

The contact system

The contact system is a proteolytic pathway activated when coagulation factor XII (FXII), high molecular weight kininogen (HK) and plasma kallikrein (PK) get into contact with negatively charged surfaces triggering inflammation, coagulation, fibrinolysis and the complement system [29]. *In vivo*, the contact system can be activated by several endogenous molecules, such as RNA, DNA, Nucleophile Extracellular Traps (NETs) and Polyphosphates (PolyP), released from activated platelets. For *in vitro* studies, the contact system is often triggered by the addition of exogenous compounds such as kaolin [30,31], ellagic acid [32] or the polysaccharide dextran sulfate (DXS)[33,34].

Activation of FXII

FXII is the central serine protease of the contact system. It is mainly synthesized by liver hepatocytes and circulates in the blood plasma as a 596 residues long zymogen. When in contact with polyanionic surfaces, it undergoes auto-activation by limited proteolysis of the R372 – V373 peptide bond (figure 6). Active FXII (FXIIa) is composed of two protein chains, one heavy, 353 residues long, and one light with 223 residues, connected by a disulfide bond between C359 and C486[35,36]. The surface and protein binding heavy chain contains two fibronectin binding domains, two EGF domains, one

Kringle domain and a proline rich domain. The active center with the catalytic triad (H412, D462 and S563) sits in the light chain.
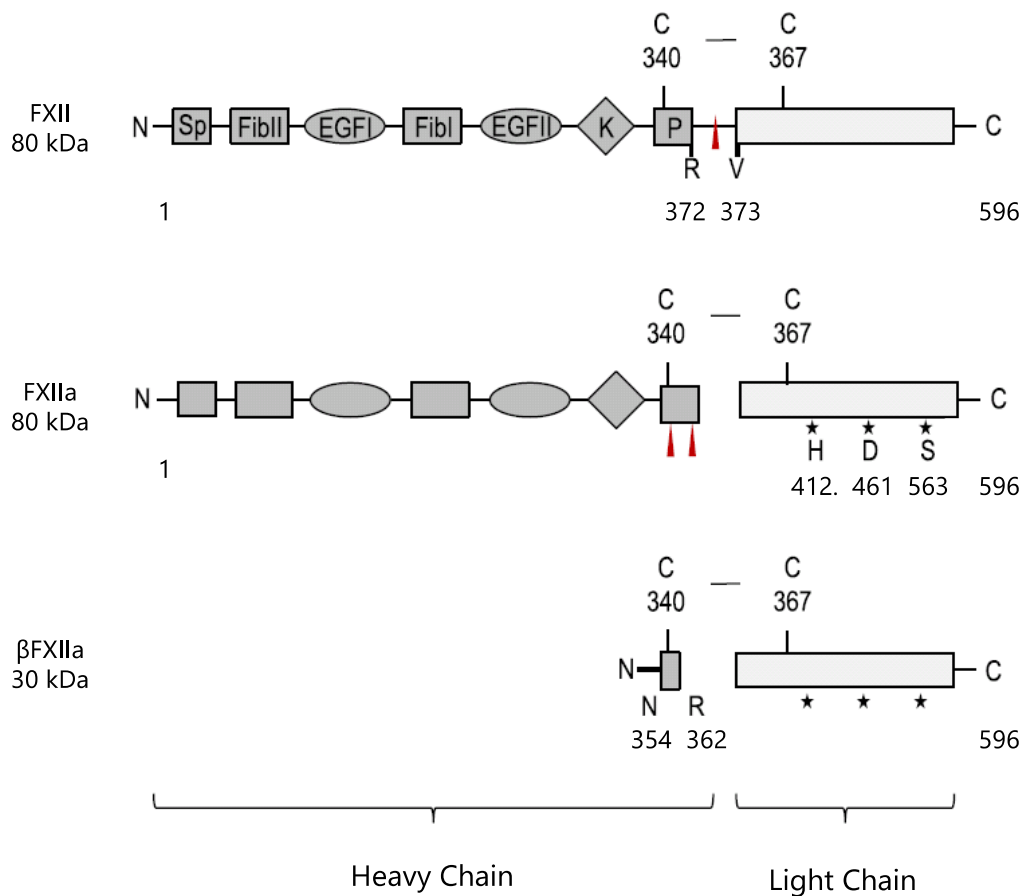

Figure 6: Schematic representation of factor XII (FXII) and its proteolytic species. Proteolytic cleavage sites are indicated by red arrows The FXIIa heavy chain contains 5 domains (FibI, FibII, EGFI, EGFII and Kringle (K)) as well as a proline-rich region (P) and binds to negatively charged surfaces. The light chain contains the catalytic triad D461, H412 and S563 marked with *[37].

Once factor XII is activated, it is able to hydrolyze the R390 – I391 peptide bond from plasma pre-kallikrein (PPK) to generate the active serine protease plasma kallikrein (PK)[38]. Active PK consists of two chains connected by a disulfide bond. The 370 residues long (50 kDa) heavy chain contains four apple domains for protein-protein interaction with the substrates. The light chain consists of 247 residues (30 kDa) and contains the catalytic triad (H434, D483 and S578). PK cleaves FXII to produce FXIIa, thereby enhancing FXII activation in a positive feed-back-loop (figure 7). Furthermore, it circulates bound to high molecular weight kininogen (HK). Upon activation by FXIIa, PK

cleaves HK at R389 – S390 and K379 – R380 to release the peptide hormone bradykinin (BK). BK then triggers an inflammatory pathway via G-protein coupled bradykinin receptor (BR2), causing vasodilatation, swelling, and pain[39]. The remaining HK is constituted of two chains of about 55 kDa linked by a disulfide bond[40].
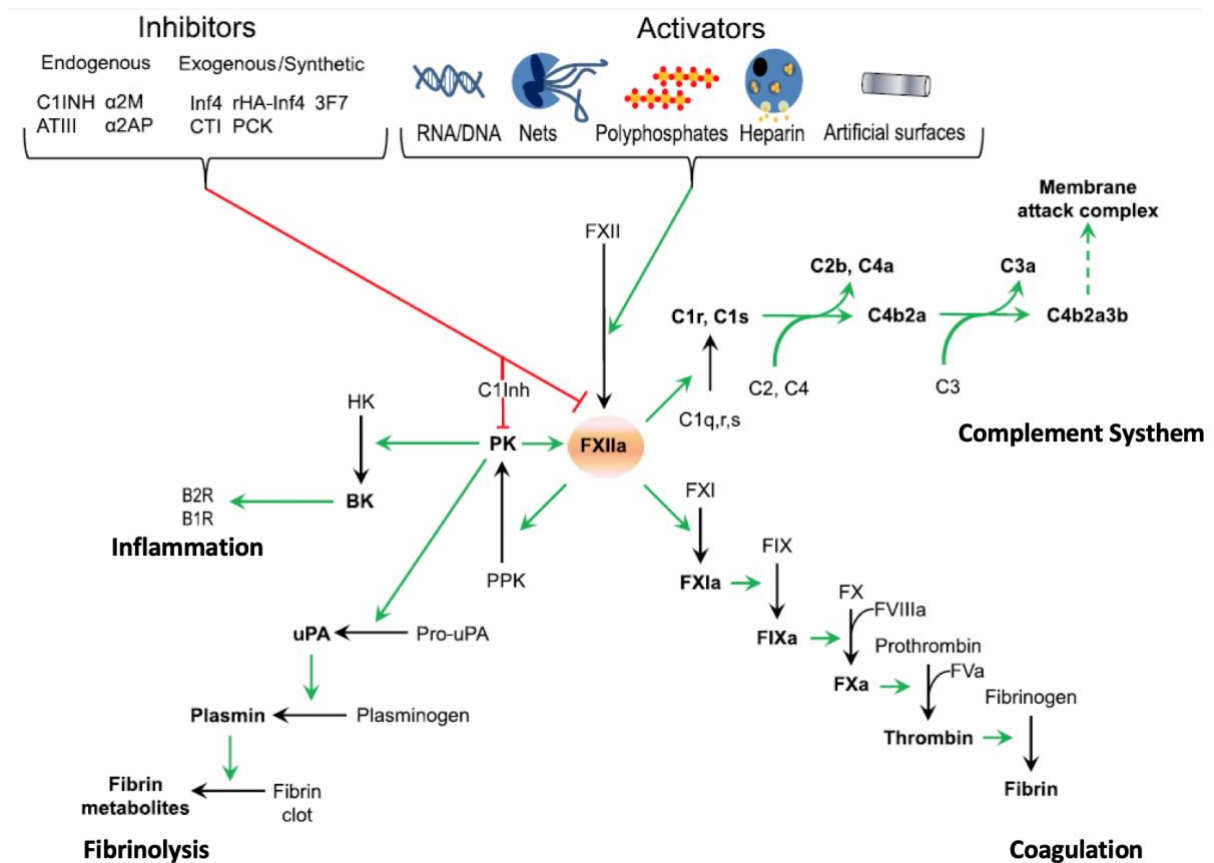

Figure 7: Pathways of the contact system. After activation by negatively charged surfaces FXIIa activates four different pathways: a) The inflammation kallikrein-kinin pathway by converting plasma pre-kallikrein (PPK) into active plasma kallikrein (PK), which cleaves high molecular weight kininogen (HK) to bradykinin (BK). The latter binds to kinin receptors (B2 and B1 receptors) and triggers inflammation. b) The complement system by activation of the C1qrs complex subunits C1r and C1s leading to formation of the membrane attack complex. 3) Fibrinolysis upon activation of pro-urokinase into urokinase, that in turn cleaves plasminogen to produce plasmin, to degrade fibrin clots. d) The intrinsic coagulation pathway by FXIa formation, thrombin activation and fibrin generation. The contact pathway is controlled mainly by C1 inhibitor (C1-inh) that inhibits both FXIIa and PK. Activation is represented by green arrows and red arrows indicate inhibition. Proteins in bold represent the result of proteolytic cleavage of their precursors[37].

Coagulation is triggered by two pathways: the extrinsic pathway, regulated by factor VII (FVII) and the intrinsic pathway, regulated by FXIIa. FXIIa cleaves the peptide bond R387 – I388 of FXI. A series of proteolytic events end with the cleavage of pro-thrombin

into thrombin and fibrinogen into fibrin into cross-linked fibrin, consequently leading to clot formation. The dissolution of the fibrin clot is called fibrinolysis. Pro-urokinase-type plasminogen activator (pro-uPA) is a substrate for PK. The proteolytic cleavage of the peptide bond K177 – I178 produces the active uPA that in turn cleaves the zymogen plasminogen into plasmin, ultimately activating the pathway of fibrinolysis. Meaning, that contact system activation of FXII leads to coagulation and clot dissolution. A balance of these two pathways is essential for hemostasis. The involvement of FXII in hemostasis was neglected by the scientific community, since patients with FXII deficiency demonstrated no abnormal bleeding during injury[38,41]. Nevertheless, more recent studies have shown that FXII activation by platelet released Polyphosphates (PolyP) has a strong role in thrombosis [42]. PolyP is a linear polymer of phosphoric acid monomers linked by high-energy phosphoanhydride bonds [43]. It is present in platelets at various chain lengths and released upon their activation. Longer chains of PolyP provide the negatively charged surface needed for FXII activation[44].

Several compounds have been used to study the activation of the contact system. Depending on the activating molecule, different pathways can be triggered and are summarized in the table below.

Table 4: Effects of contact system activators on the *in vivo* and *in vitro* Factor XII-dependent coagulation and inflammation pathways[35].

Compound	In Vitro Effect		In Vivo Effect	
	Intrinsic Coagulation Pathway	Kallikrein-Kinin System	Procoagulant	Proinflammatory
Nonphysiological materials				
Glass	+	+	+	+
Kaolin	+	+	+	+
Ellagic acid	+	+	−	+
Dextran sulfate (high molecular weight)	+	+	−	+
Ellagic acid	+	+	−	+
Oversulfated chondroitin sulfate	−	+	−	+
Poly I:C	+	+	+	?
Biomaterials				
Dialysis membranes				
Cuprophane/Polyacrylonite/AN69 for example	+	+	+	+
Vascular grafts				
(Dacron/PTFE/ PDMS)	+	+	?	?
Metal (steel/titanium/aluminum)				
Therapeutical compounds	+	+	?	?
Aptamers	+	+	?	?
Iron oxide nanoparticles	?	+	?	+
Endogenous substances				
Glycosaminoglycans	−	+	?	?
Nucleic acids (RNA, DNA)	+	+	?*	?
Sulfatide	+	+	+	+
Urate crystals	+	+	?	+
Misfolded protein aggregates	−	+	−	+
Polyphosphates	+	+	+	+
Amyloid β peptide	−	+	−	+

*Administration of RNAse that degrades RNA provides thromboprotection in mice.

Inhibition

The major inhibitor for FXII is the C1-esterase inhibitor (C1-inh). This 105 kDa glycoprotein is produced by the liver and secreted into the plasma at a concentration of 250 μg/ml. The C1-inh belongs to the serpins[45]. This inhibitor presents the R466 – T467 peptide bond as a substrate to the catalytic triad of FXII. During hydrolysis of the bond the C1-inh undergoes a rapid conformational change and remains covalently bound to the catalytic S from FXII. Due to its covalent bond to its target, the C1-inh constitutes a suicide inhibitor. With the same mechanism it is also a potent inhibitor for PK, FXIa and the proteases of the complement system[46] . Other endogenous protease inhibitors have been described to inhibit FXII, namely α2-Antiplasmin, α2-Macroglobulin and antithrombin III, but with a much lower (about 150 times) specificity.

Contact system and disease

Several health conditions have been described to be related to proteases of the contact system. Namely, thrombosis, hereditary angioedema (HAE), sepsis, inflammation and allergy.

Hereditary angioedema

HAE is the most prominent example of complications related to the contact system. This condition is characterized by sudden painful swelling of the face or limbs and can become life threatening when it involves the intestine or the upper airways. There are three types of HAE: I) is caused by low levels of C1-inh, II) by dysfunctional C1-inh and III) is caused by mutations of the F12 gene. All of the above result in an overactivation of FXII, due to absence of inhibitor or overactive FXII protease activity. The endogenous trigger is the activation of the contact system. FXII gets activated, rapidly resulting in the activation of PK and the consequent release of BK from HK. In a healthy individual, this proteolytic cascade is rapidly quenched by the C1-inh. Individuals with HAE lack the ability to stop the inflammatory process by inhibition of FXII, ending up in extreme swelling due to excessive release of BK. Alongside with small trauma, administration of estrogens, angiotensin converting enzyme inhibitors or angiotensin receptor antagonists are probable causes for the initiation of such episodes[47]. Until recently there were no specific treatments for HAE. Acute episodes were treated by intravenous administration of C1-inh, B2R antagonists and Kallikrein inhibitors. In case of acute swelling of the airways, intubation or tracheotomy are applied[48,49]. Antibodies against FXII[50] and kallikrein are in development, but have not yet been approved for clinical use.

Thrombosis

A thrombus is the occlusion of a blood vessel formed by the aggregation of circulating blood cells (mostly platelets) and plasma proteins, such as thrombin. According to Virchow's triad, stasis (blood flow, sheer forces), endothelial injury and hypercoagulability are the main factors influencing thrombosis[51]. Upon injury, platelets

are recruited and activated to promote coagulation, preventing excessive blood loss. On the other hand, fibrinolysis is activated in order to dissolve the clot and restore normal blood flow. Activation of the contact system promotes coagulation via the intrinsic pathway, but also contributes to fibrinolysis via PK-mediated urokinase-type plasminogen activator (uPA) activation and is therefore strongly involved in homeostasis. FXII deficient individuals do not suffer from any bleeding disorders, but it has recently been discovered that they are protected against thrombosis[52] (figure 8). It has also been shown that targeting the FXIIa-FXI axis of the pathway interferes with the fibrin formation at the thrombus and increased embolization (thrombus fragmentation into smaller particles).
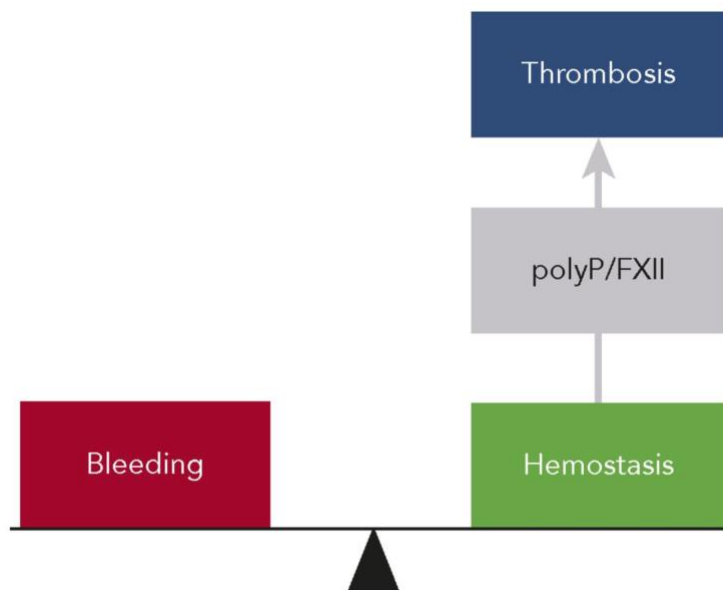

Figure 8: FXII/PolyP driven thrombosis does not impact hemostasis. Activated platelets in the thrombus release PolyP, inducing the intrinsic pathway of coagulation via FXII activation. Inhibition of FXII interferes with coagulation in the thrombus, reducing its formation without interfering with hemostasis[42].

PolyP released from active platelets within the thrombus activate FXII and contribute to pathologic coagulation and therefore thrombus growth. One of the most common treatments to prevent or treat thrombosis is the administration of anticoagulating agents such as heparin or coumarins. Administration of these compounds significantly interferes with hemostasis, increasing the risk for bleeding[53]. Specifically targeting FXII,

however, has become of increasing interest for thrombosis prevention. Development of these agents promises thrombosis prevention without increasing the risk of bleeding.

Aim

The plasma contact system is a complex cascade involving several proteases and their respective inhibitors. Its activation results in coagulation, inflammation, thrombosis and fibrinolysis. The classical bottom-up approach to analyze proteins is not suited to elucidate the proteolytic mechanisms involved in the contact system, since the different protein species cannot be distinguished after tryptic digestion. Kwiatkowski et al. have shown that combining LC-MS/MS with SDS-PAGE to generate migration profiles can be used to evaluate proteolytic processing of proteins[54].

It has been shown that coagulation by FXII is only activated in the presence of PolyP and not in the presence of DXS, whereas both activators result in the formation of bradykinin.

It is hypothesized that 1) the FXII activation by PolyP and by DXS results in a different substrate specificity of activated FXII and 2) as a result of the different substrate specificity, different proteins interact with FXII and are consequently activated. Therefore, this thesis aims at the clarification of the molecular mechanisms underlying the activation of the different pathways triggered by PolyP and DXS induced FXII activation. The migration profile assay will be used to identify the protein species of FXII, its downstream proteases and their inhibitors produced upon activation by DXS and PolyP.

Results

Suitability of migration profiles to study the contact system

In a first pilot experiment, the suitability of the migration profile assay, developed by Kwiatkowski et al.[54], was tested for the study of the FXII activation mechanism. Since the conversion of the FXII zymogen into the active species FXIIa results from its proteolytic cleavage. Thus, activation of the contact system should result in the identification of a FXII-species in bands corresponding to lower molecular weights. Therefore, plasma was incubated with the known contact system activator DXS and applied onto an SDS-page, together with a control sample of plasma incubated with PBS. The proteins of the 19 bands from each lane of the gel (figure 9) underwent bottom-up protein analysis by LC-MS/MS, resulting in a total of 38 datasets. Each dataset is comprised of a total ion chromatogram (TIC) represented in figure 10.
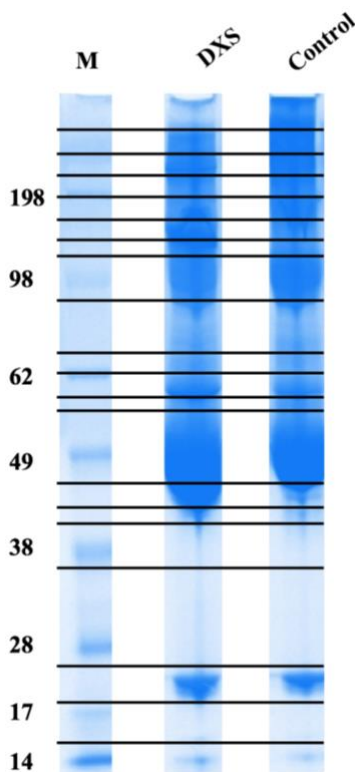

Figure 9: SDS-Page from plasma samples after incubation with dextran sulfate (DXS) and PBS (control). The relative molecular weight is represented by the marker (M). 15 µg of protein were loaded onto a 10% polyacrylamide gel and separated by 140 V. Proteins were stained with Coomassie blue. Horizontal lines represent cutting pattern by witch each lane was divided for protein identification.
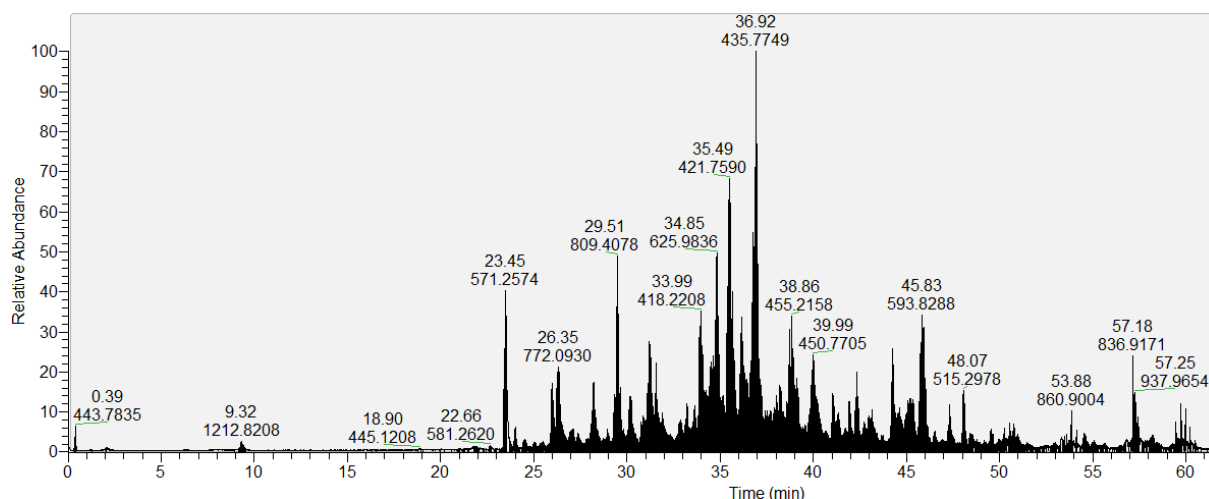
Figure 10: Total ion current chromatogram (TIC) from the LC-MS/MS analysis from the 90 kDa SDS-page band.

Behind each signal in that chromatogram lies a full-scan spectrum of the eluting peptides at each time point followed by their corresponding fragment spectra (figure 11). The spectral information is used to assess the identity of the peptide via database search. Therefore, the m/z value of the intact peptide is matched to the m/z value of all theoretical peptides originating from the *in-silico* digestion of a FASTA database. After that, the signals of the corresponding fragment spectrum are matched to the theoretical spectra for identification.

Once the proteins were identified, the extracted ion chromatograms (EIC, figure 12) from the peptides were used to construct migration profiles. Therefore, for each identified peptide ion the EIC was generated and the relative intensity (area under the curve, AUC) was calculated. The obtained AUC was then plotted against the respective molecular weight in the SDS-Page as shown in figure 13 by the example of the unique peptide VVGGLVALR from FXII light chain.
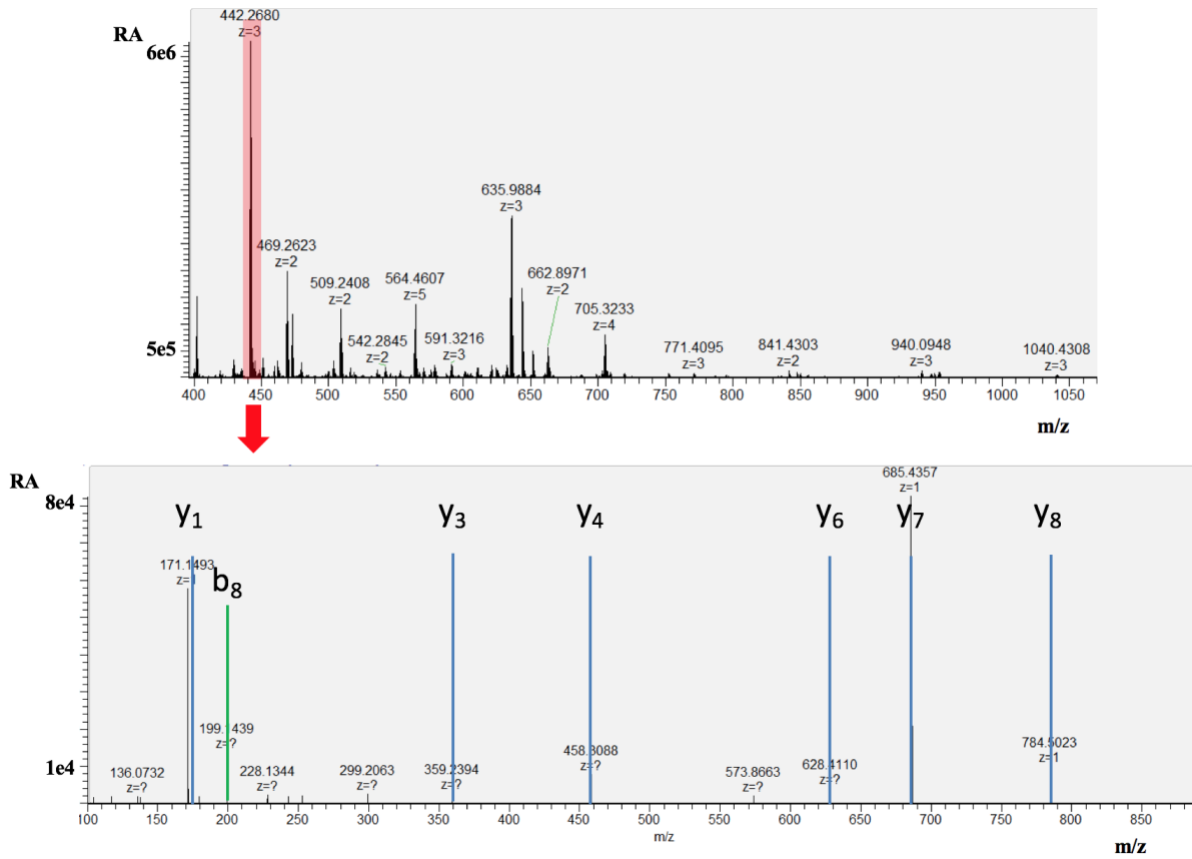
Figure 11: Full-scan spectrum and corresponding fragment spectrum from the VVGGLVALR peptide from FXII. The full scan spectrum entails all molecules eluting from the column at 43 min. Below is the fragment spectrum from the precursor with an m/z of 442.26 annotated with the y and b ions leading to the identification of the peptide.
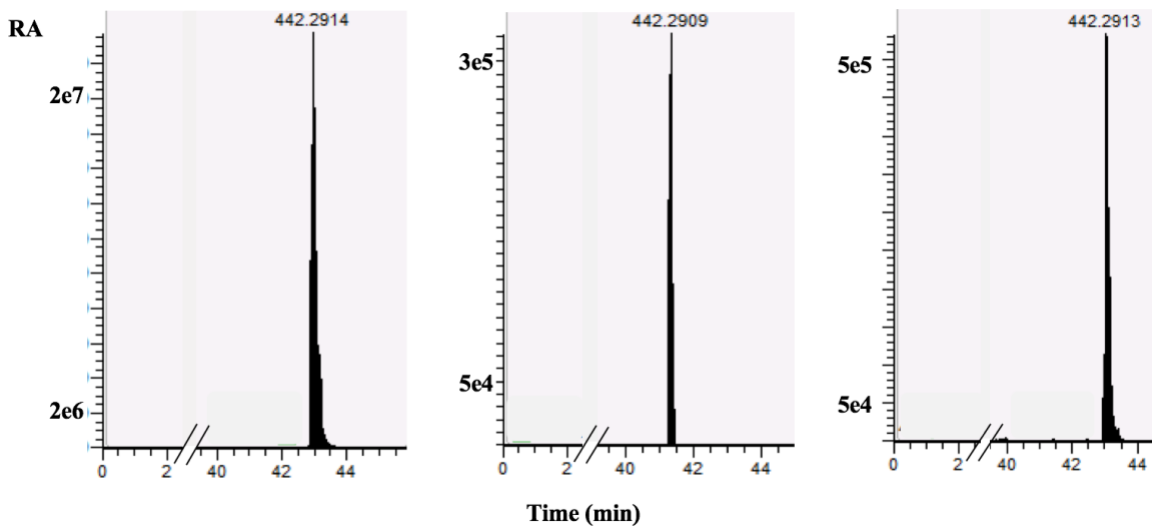

Figure 12: Extracted ion chromatograms from the VVGLVAR peptide found in SDS-page bands corresponding to 90kD, 50 kDa and 38 kDa from plasma after incubation with dextran sulfate (DXS).
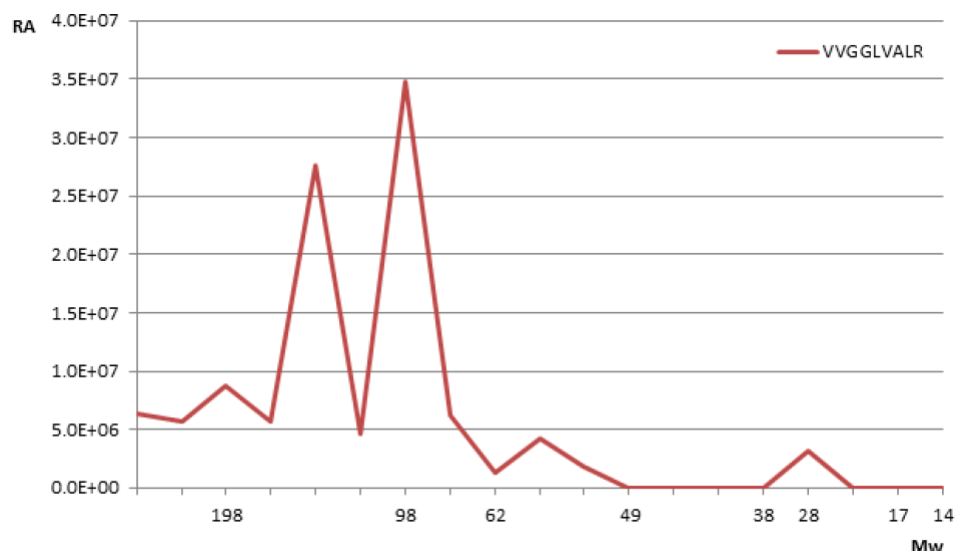
Figure 13: Migration profile of the VVGGLVALR from FXII after incubation od plasma with DXS. The relative abundance calculated from the EIC is plotted against the empirical molecular weight from the SDS-Page.

This method demonstrates relative abundance of a peptide in relationship to a position in the gel, which can be correlated to a molecular weight. In the case of a conversion of a protein species into a new one, e.g. by its proteolytic processing, which results in a change of the molecular weight, the new species will appear at a different position in the gel. In the case of the addition of a molecule via the formation of a covalent bond, the new species will appear in a band corresponding to a larger molecular weight compared to the original species.

The obtained migration profiles for FXII show significant differences between the activated species (FXIIa) and the non-activated species of FXII (figure 14). Before incubation with DXS, FXII was detected in a band at approximately 90 kDa, which corresponds to the molecular weight of the full length FXII. In that band, most peptides were identified at highest intensity in both samples (control and incubation with DXS). Incubation of plasma with DXS resulted in the proteolytic activation of FXII and, consequently the detection of the heavy chain in a separate band from the light chain under the reducing conditions of the SDS-page. This newly formed species, the heavy chain, was detected in the band corresponding to 40 kDa (figure 14 – bottom).
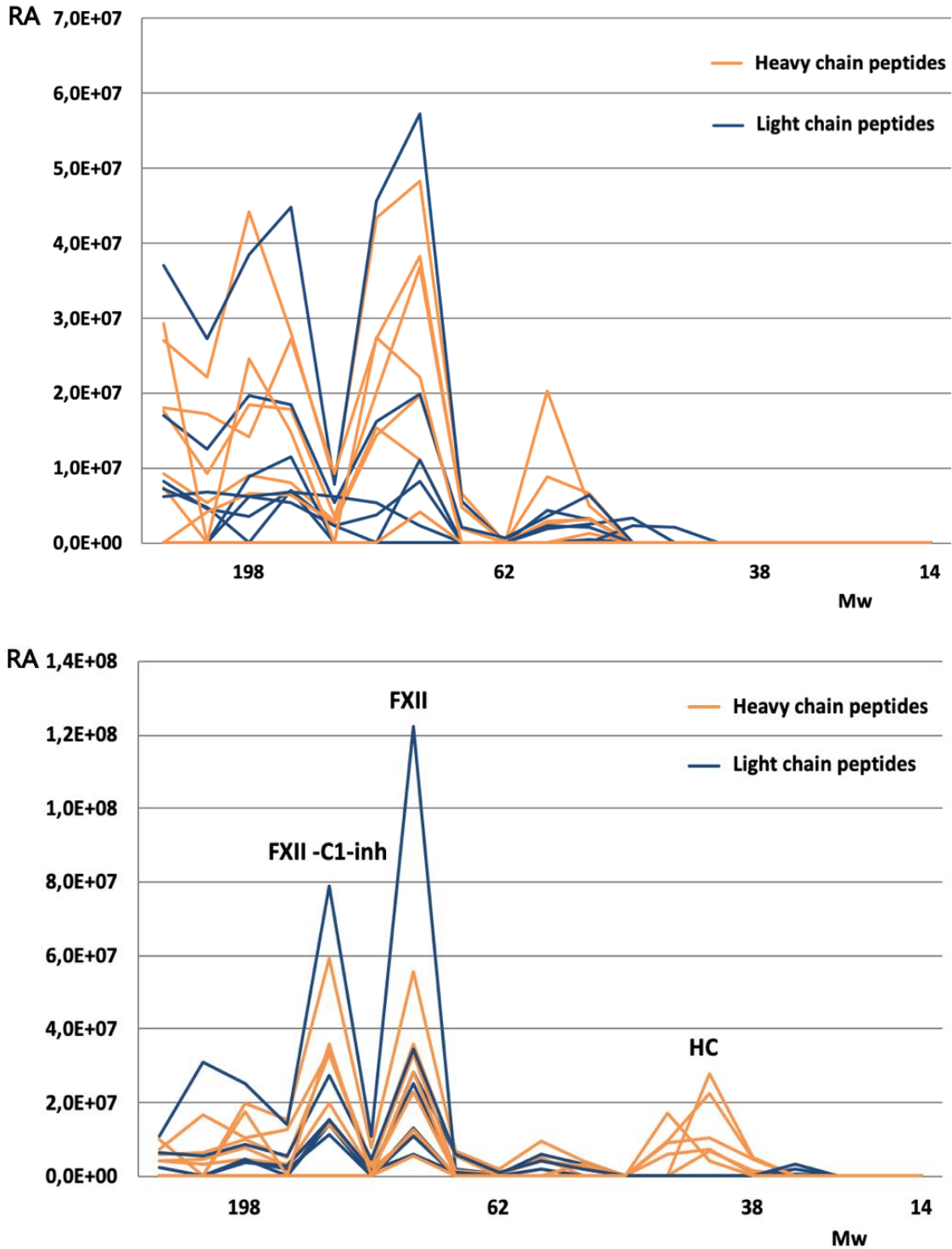
Figure 14: Migration profiles of factor XII species. Top: As a control, plasma was incubated with PBS. Bottom: plasma was incubated with DXS (0.04 µg/ml in PBS). Plasma proteins were separated by SDS-Page and 19 individual bands from each sample underwent proteome analysis. The relative abundance (RA, in a.u.) of each peptide is plotted against the empirical molecular weight (Mw, in kDa). Each colored line represents a different tryptic peptide. Blue peptides belong the FXII light chain (residue 20 – 372) and orange peptides result from the FXII heavy chain (residue 373 – 615)

A larger FXII species appeared in a band above at approximately 180 kDa. This species can be explained by the covalent binding of C1-inh to the proteolytic active species of FXIIa. C1-inhibitor has an empirical molecular weight of about 100 kDa, once it is covalently bound to FXIIa's light chain, it will no longer be separated resolved under the reducing conditions of the SDS-page and result in a signal at about 180 kDa. The plot of the migration profile of the C1-inh is shown in figure 6. Comparing the migration profile before and after incubating plasma with DXS, the appearance in the latter sample of a C1-inhibitor species at about 180 kDa is obvious. The signal is found in the same band as the signal of the increased molecular weight FXII species, evidencing the formation a new protein species, consisting of FXII and C1-inh. This was formed after proteolytic activation of FXII, which was inhibited by binding covalently to the C1-inh. The FXII-C1-inh species was not detected in the control sample (figure 15-bottom).
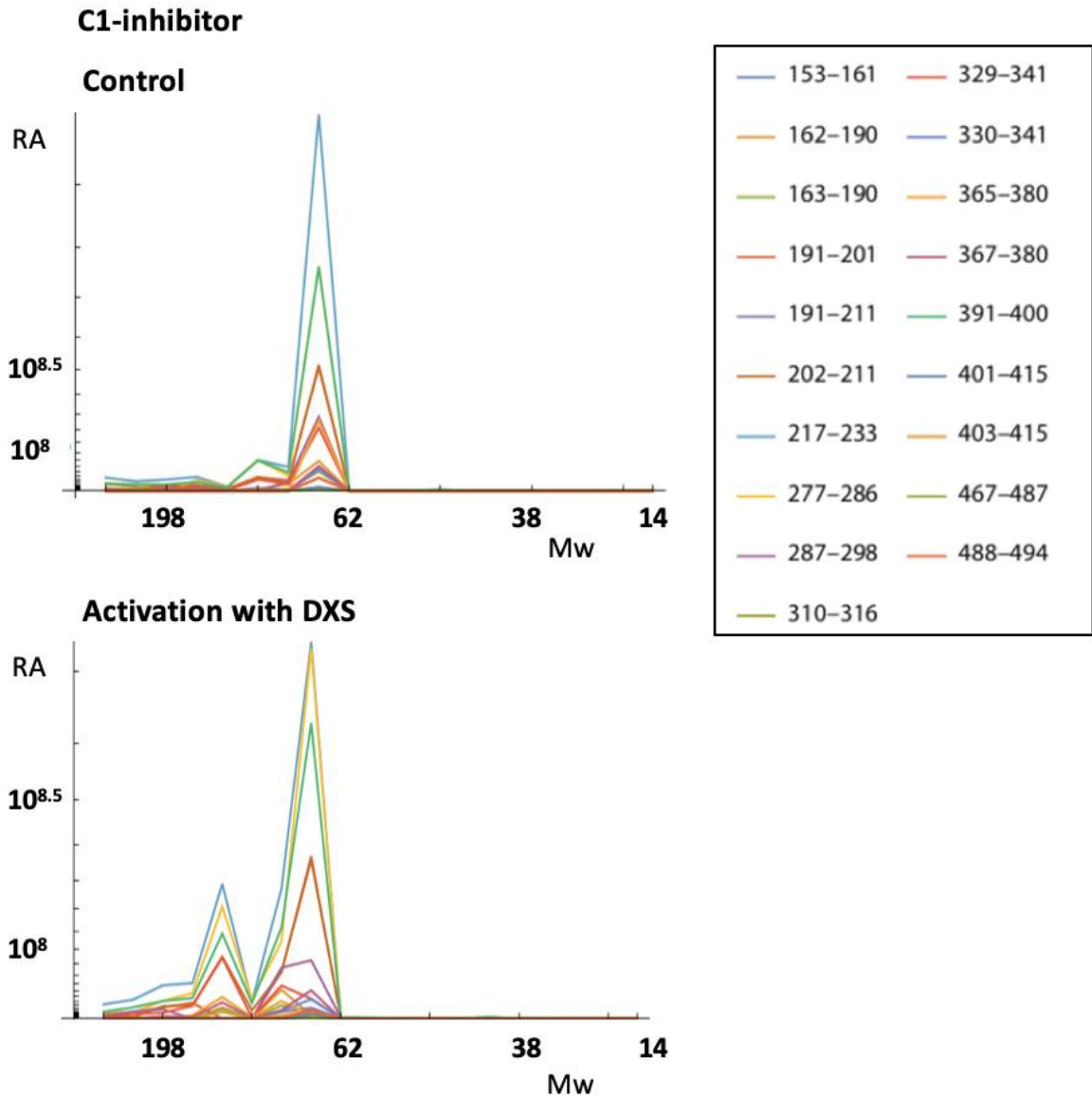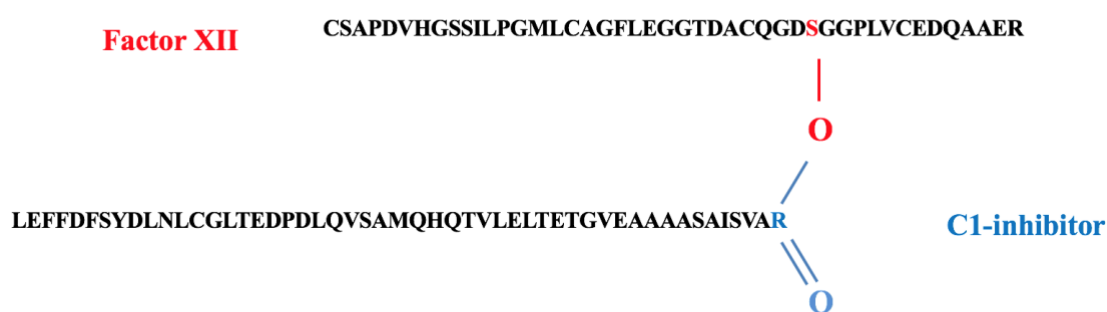
Figure 15: Migration profile of C1-inh species. Top: As a control, plasma was incubated with PBS. Bottom: plasma was incubated with DXS (0.04 µg/ml in PBS). The relative abundance (RA, in a.u.) of each peptide is plotted against the empirical molecular weight (Mw, in kDa). Each colored line represents a different tryptic peptide (amino acid positions shown in the legend – top right).

The tryptic digestion of the FXII-C1-inh complex generates a peptide consisting of a peptide chain from FXIIa and a peptide chain from C1-inh covalently bound by the reactive serine (figure 16). This large molecule was not identified in any of the experiments. It can be hypothesized that this is due to irreversible binding to the C18 chromatographic material of the column or it being outside the set MS scan window. The theoretical charge of the covalently bound peptides at pH 2.3 was calculated, adding a positive charge for each basic amino acid and N-terminal and a negative

charge for each phosphorylation and acetylation[55]. According to these calculations the molecule is five times positively charged and, would accordingly have an m/z of 1987.91, therefore being outside the set m/z range of the full scan window (400 – 1500). Being constituted by 45 and 51 amino acids each, the peptides from FXII and C1-inh were also not identified when not covalently bound.

Factor XII   CSAPDVHGSSILPGMLCAGFLEGGTDACQGD**S**GGPLVCEDQAAER

O

LEFFDFSYDLNLCGLTEDPDLQVSAMQHQTVLELTETGVEAAAASAISVA**R**   **C1-inhibitor**

O

Mw=9934,57 Da

Figure 16: Simplified molecular structure of the covalently bound tryptic peptides of FXII and C1-inh. The reactive R444 from C1-inh binds covalently to the reactive S from FXII, permanently inhibiting it. After tryptic digestion and under reducing conditions the peptides remain bound, resulting in a molecule with 9.934 kDa. Theoretically, at pH 2.3, this molecule carries five positive charges, for the tree basic amino acids and the two N-termini.

The results of the pilot-experiment show that with the migration profile assay not only proteolytic processing of proteins can be followed, but also the formation of fusion protein species like C1-inh-FXII, consisting of the protease and its inhibitor.

Differential contact system activation

In order to understand the molecular mechanisms behind the differential activation of FXII by DXS and PolyP the migration profile assay was applied. Therefore, plasma samples were incubated with one of the two molecules. As a negative control plasma was incubated with PBS. In order to limit the analysis to proteins interacting directly with FXII or recruited due to the presence of the negatively charged surfaces following the incubation, an enrichment by immunoaffinity chromatography with an antibody against FXII was performed. The enriched proteins were separated by SDS-page (figure 17) and migration profiles were constructed for all 415 identified proteins in an automated script.
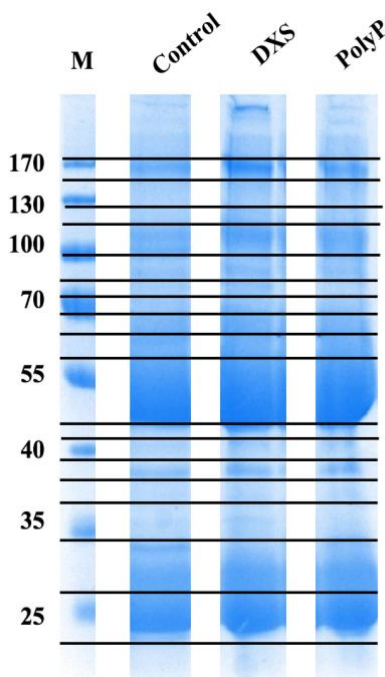

Figure 17: SDS-Page of the eluates of a FXII-antibody-immunoprecipitates of plasma samples incubated with dextran sulfate (DXS) or Polyphosphate (PolyP). As a control, untreated plasma was used. The relative molecular weight is represented by the marker (M). Proteins were stained with Coomassie blue. Horizontal lines represent cutting pattern by which each lane was divided for protein identification.

It is notable that within the band corresponding to a molecular weight of about 65 kDa (figure 18) mainly serum albumin was identified. The migration profile of this protein remains unchanged before and after incubation with either of the used contact system activators. A residual amount of peptides belonging to serum albumin were identified

in bands corresponding to lower molecular weights. The incubation of the samples at 37 °C might have contributed to some unspecific proteolytic degradation of the plasma proteins, resulting in lower molecular weight species. Serum albumin peptides found at higher molecular weights may represent possible aggregations. The migration profile of serum albumin remained identical after activation with either of the used FXII activators. This protein is abundant in plasma with no role in the contact system or another proteolytic pathway, thus serving as an internal control for this experiment and being an example for unspecific binding.
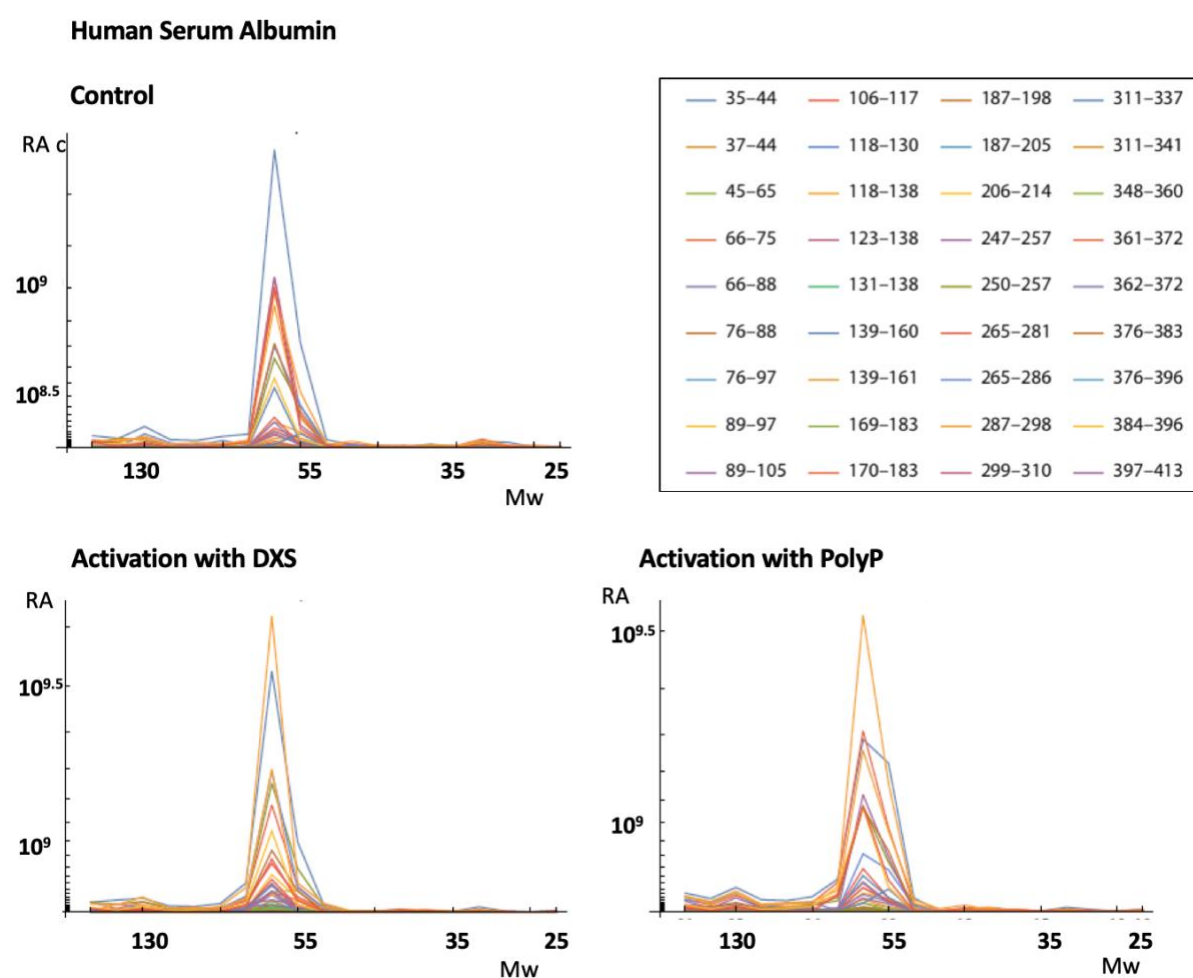

Figure 18: Migration profiles of human serum albumin. The relative abundance (RA, in a.u.) of each peptide is plotted against the empirical molecular weight (Mw, in kDa). Each colored line represents a different tryptic peptide (amino acid positions shown in the legend – top right)

Activation of the inflammation pathway by PolyP and DXS

The migration profiles of FXII, before and after incubation with DXS and PolyP, inducing a contact system activation, are clearly distinguishable (figure 19). In the control sample only one FXII species was seen, since it remained intact, hence all identified FXII peptides remained at the band corresponding to approximately 80 kDa. The sample incubated with DXS shows a small amount of FXII peptides in the band corresponding to 80 kDa and many peptides were identified in bands corresponding to lower molecular weights, indicating proteolytic processing of FXII into species of lower molecular weight. After incubation of plasma with PolyP the most abundant FXII species identified was the intact FXII, as the majority of the identified peptides appear at a molecular weight of 80 kDa. A small amount of the cleaved species, consisting of peptides from the FXII-heavy chain is produced, shown by the signal at 35 kDa. The small signal at 130 kDa arises from a small portion of FXII being covalently bound to C1-inh. At a first, the analysis of these FXII migration profiles would suggest that FXII is only activated by DXS and not by PolyP. Therefore, the migration profiles of the proteins downstream in the proteolytic cascade were also analyzed. In contrast to the control samples (figure 20A), it is noticeable that the incubation of plasma with both molecules generated different species of plasma kallikrein (figure 20 B and C). These species were not identified in the control sample.
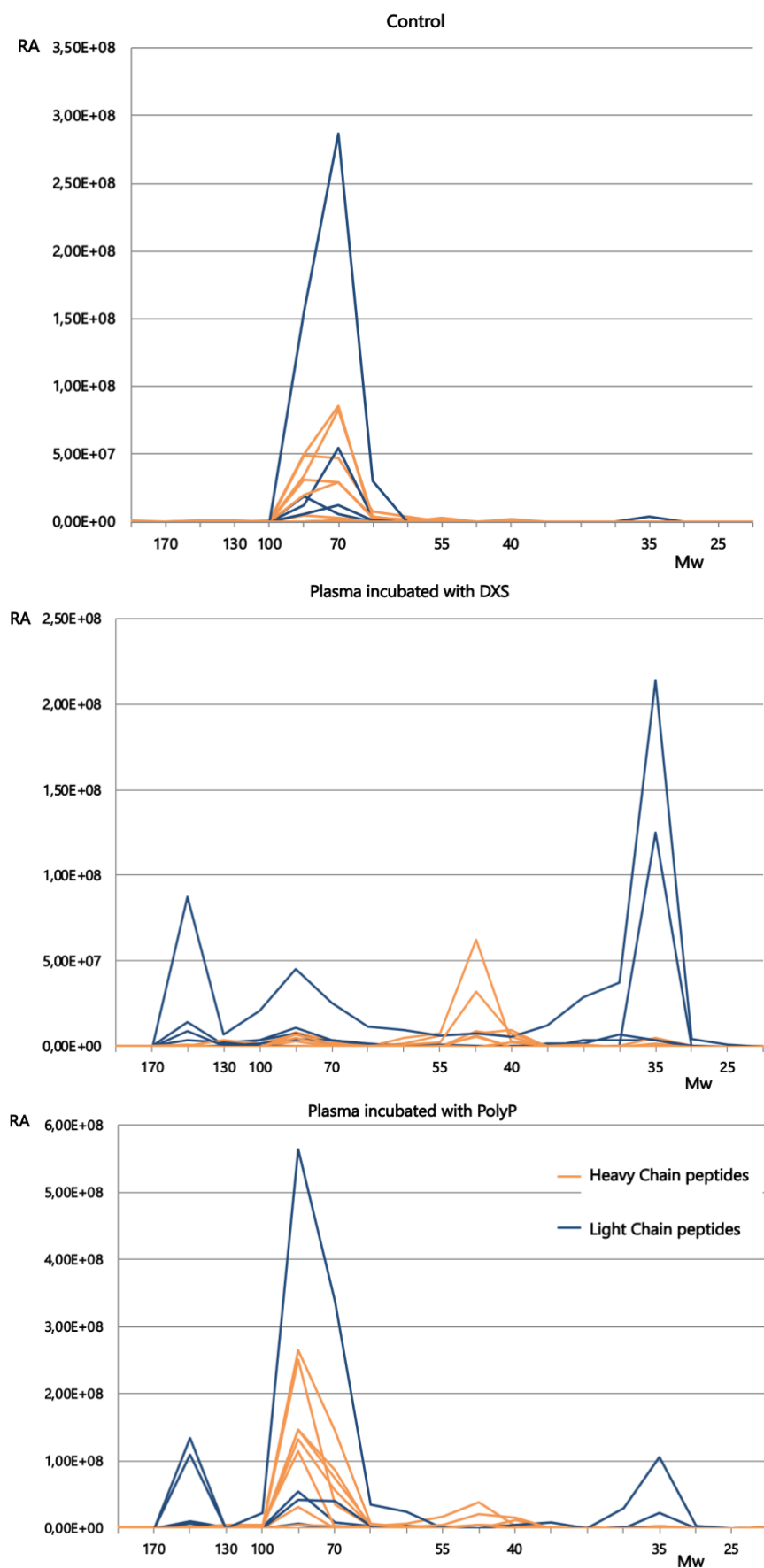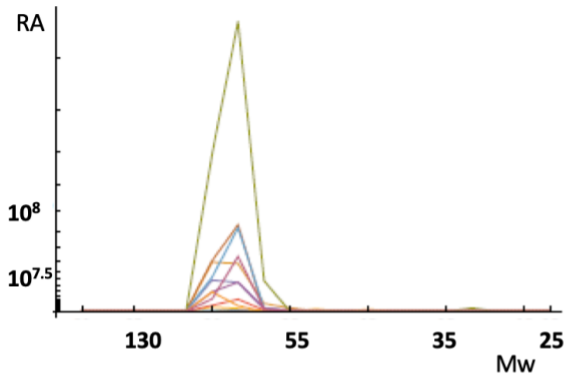
Figure 19: Migration profiles of FXII species obtained from the control sample, plasma incubated with DXS and plasma incubated with PolyP. Peptides belonging to the heavy chain are colored in orange and peptides from the light chain are represented in blue. The relative abundance (RA, in a.u.) of each peptide is plotted against the empirical molecular weight (Mw, in kDa).
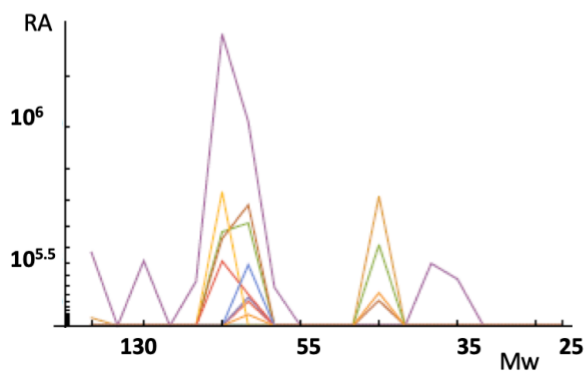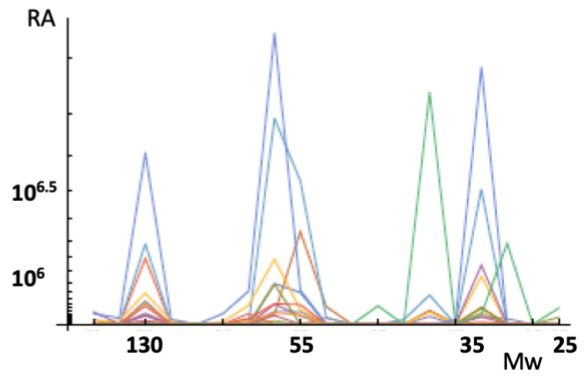
A: Control

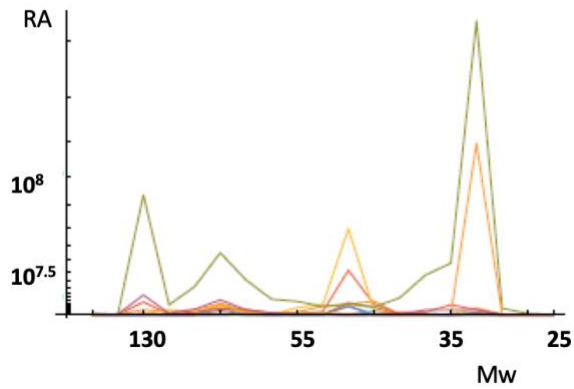**Factor XII**

Plasma Kallikrein

High Molecular Weight Kininogen
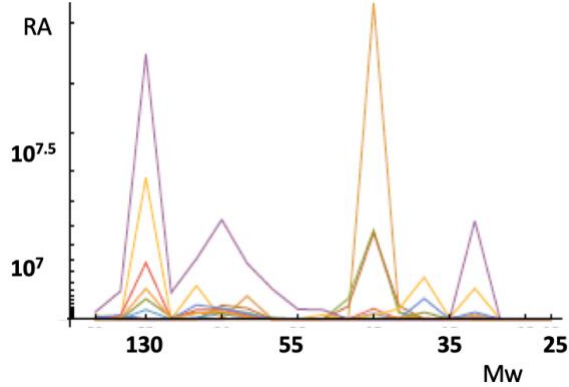

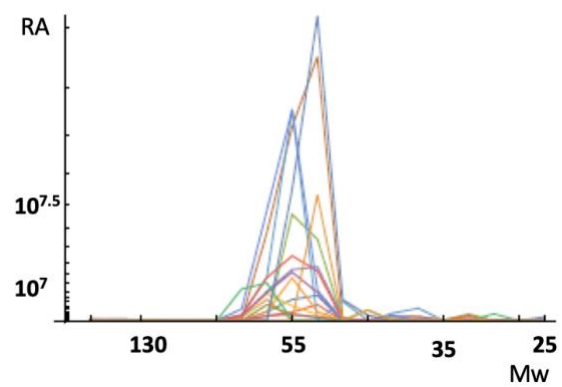**B: incubation with DXS**

Factor XII

Plasma Kallikrein

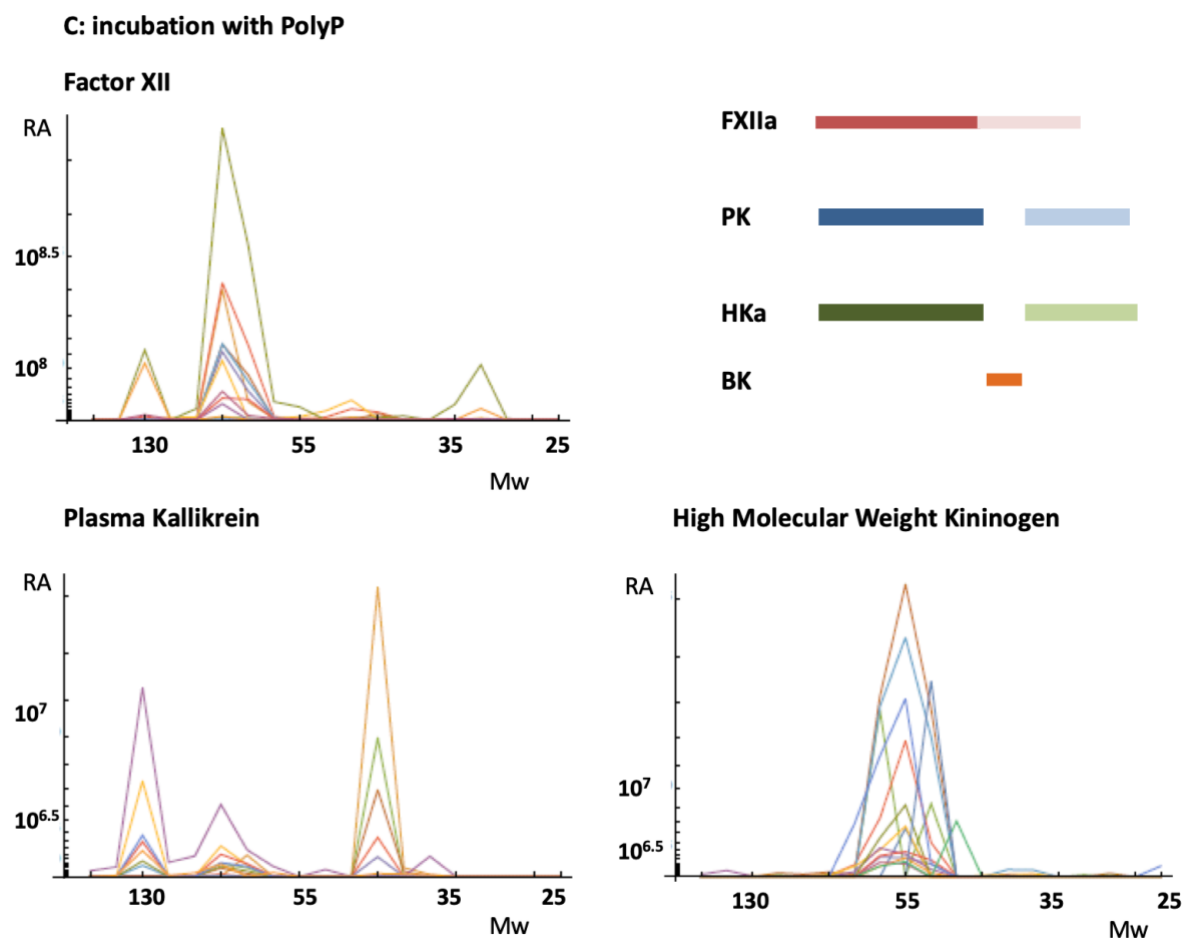

High Molecular Weight Kininogen

Figure 20: Migration Profiles of FXII, PK and HK from plasma after enrichment of FXII. The relative abundance (RA, in a.u.) of each identified peptide is plotted against the empirical molecular weight (Mw, in kDa). Each colored line represents a different tryptic peptide. A: control plasma, incubated with PBS, B: plasma incubated with DXS and C: plasma incubated with PolyP. The top right corner of each contains a schematic representation of the intact proteins or their proteolytic products inferred from the obtained migration profiles. The heavy chain of each protein is represented by the dark color (red for FXII, blue for PK and green for HK) and the light colors represent the light chain, respectively. Separately drawn chains represent proteolytic cleavage. The peptide hormone bradykinin (BK) is represented in orange. It is released from HK upon PK cleavage.

In addition to an increase of relative abundance of PK, a PK species at 130 kDa appeared as well as an increase of the relative abundance of the 40 kDa species was observed in the samples incubated with DXS and PolyP. Plasma incubated with DXS also presented a low molecular weight PK species at about 30 kDa which was not identified upon incubation with PolyP. Even more eminent was the complete conversion of the intact species of HK into its two chains (heavy and light) after proteolytic release of BK. All peptides from bands corresponding to the intact HK at

120 kDa disappeared from the migration profiles whereas the relative abundance of the peptides increased in the 55 kDa bands corresponding to the two HK chains.

These findings strongly indicate the activation of PK and that therefore FXII had been activated by PolyP and DXS. Hence, the bradykinin mediated pathway of inflammation is induced when the plasma contact system is activated by DXS and PolyP, in accordance to Maas et al. and Engel et al.[35,56], but the underlying mechanism of FXII activation is different depending on the activator molecule present.

Influence of PolyP and DXS on coagulation

The different mechanisms of FXII activation in the presence of PolyP and DXS lead to the hypothesis that the enzyme-substrate specificity of FXII and other proteins is affected. In the past it has been described that activation of FXII in the presence PolyP results in coagulation whereas in the presence of DXS it does not[35]. Therefore, all proteins involved in the coagulation cascade were screened for the generation of different molecular species upon incubation with PolyP and DXS. Several proteins involved in coagulation showed significant differences in their migration profiles depending on the activator molecule, which will be evaluated in the following sections.

Antithrombin III

Antithrombin III (ATIII) is a known protease inhibitor found in plasma[57]. This serine protease inhibitor (serpin) targets proteases from the contact activation system. The migration profiles of ATIII (figure 21) show a significant shift of the ATEDEGSEQKIPEATNR (62-78) peptide towards the FXII band (80 kDa) after incubation with DXS. This shift isn't visible in the control sample nor in the sample activated with PolyP. This peptide lies immediately before one of three known heparin biding sites (W81).

In analogy to C1-inh, the tryptic peptide from ATIII containing the reactive bond R425-S426 could not be identified. When ATIII covalently binds to FXIIa and a tryptic digestion is performed on the ATIII-FXIIa-complex a 6,7 kDa molecule is formed. The

resulting fragment spectrum would be a hybrid spectrum consisting of the fragments of one tryptic peptide from ATIII and one tryptic peptide from FXII, which cannot be identified with the standard database search used in this work.
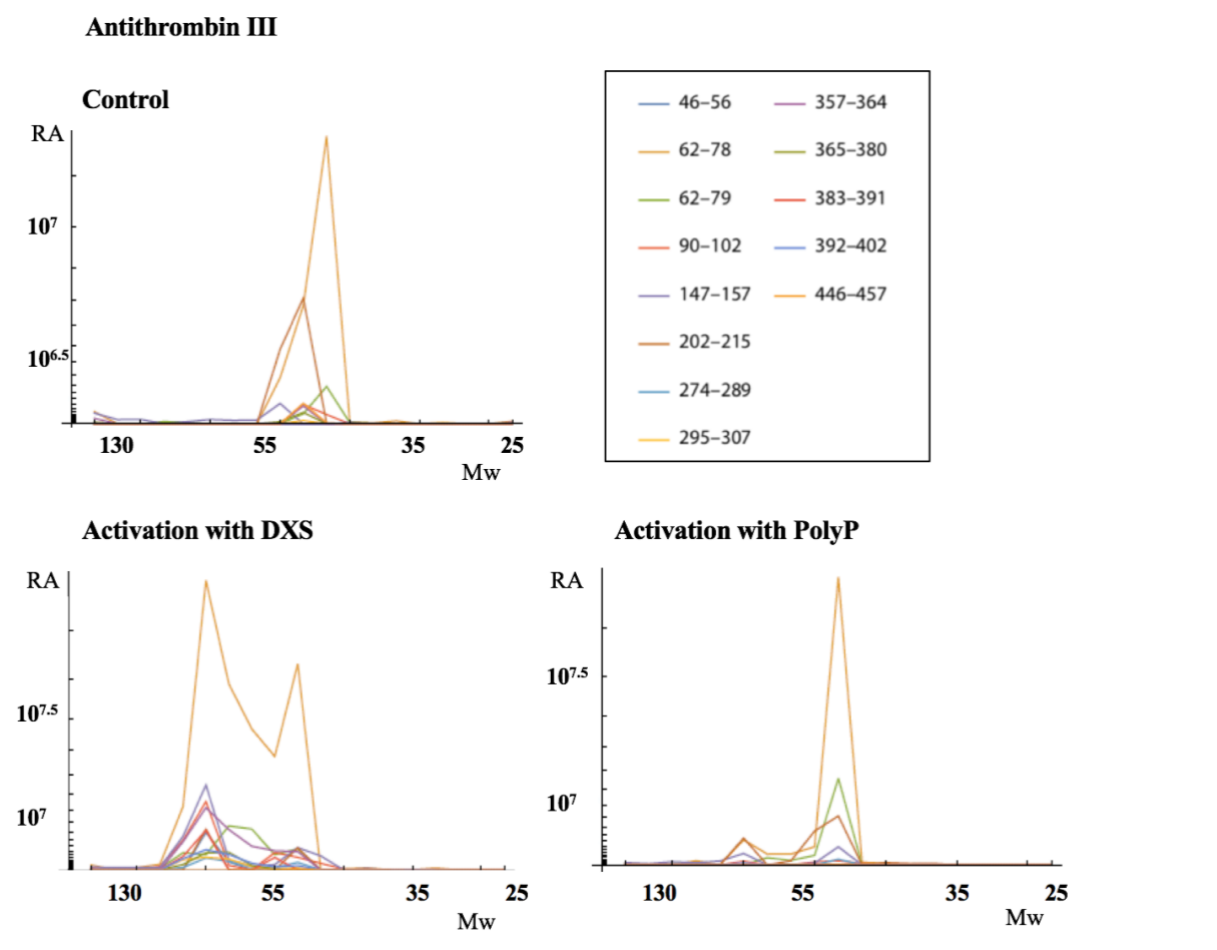
Figure 21: Migration profile of the identified Antithrombin III (ATIII) species. A total of 13 peptides were identified. The relative abundance (RA, in a.u.) of each peptide is plotted against the empirical molecular weight (Mw, in kDa). Each colored line represents a different tryptic peptide (amino acid positions shown in the legend – top right). A significant shift in the profile of the ATEDEGSEQKIPEATNR (62-79) peptide towards a higher molecular weight) is noticeable.

Hyaluronan-binding protein 2

Hyaluronan-binding protein 2 (HABP2) is a serine protease that plays an important role in fibrinolysis and to activate FVII by proteolysis[58,59]. The obtained migration profile of this protein (figure 22) in the control sample, shows an overall a lower abundance where the most abundant species has a molecular weight of above 55 kDa. The overall signal intensity of this protein increased significantly after incubation of plasma with

DXS as well as with PolyP and consequent enrichment for FXII. This indicates that HABP2 is a direct or indirect binding partner for FXIIa. Also, the migration profiles of this protein differ in dependence of the used FXII activating molecule. Whereas all identified peptides remained in the band above 55 kDa after activation of FXII with DXS, two more smaller species of HABP2 were detected at 50 kDa and 27 kDa after FXII is activated with Polyp. This indicates that, from these two activators, only PolyP seems to induce proteolytic processing of hyaluronan-binding protein 2.

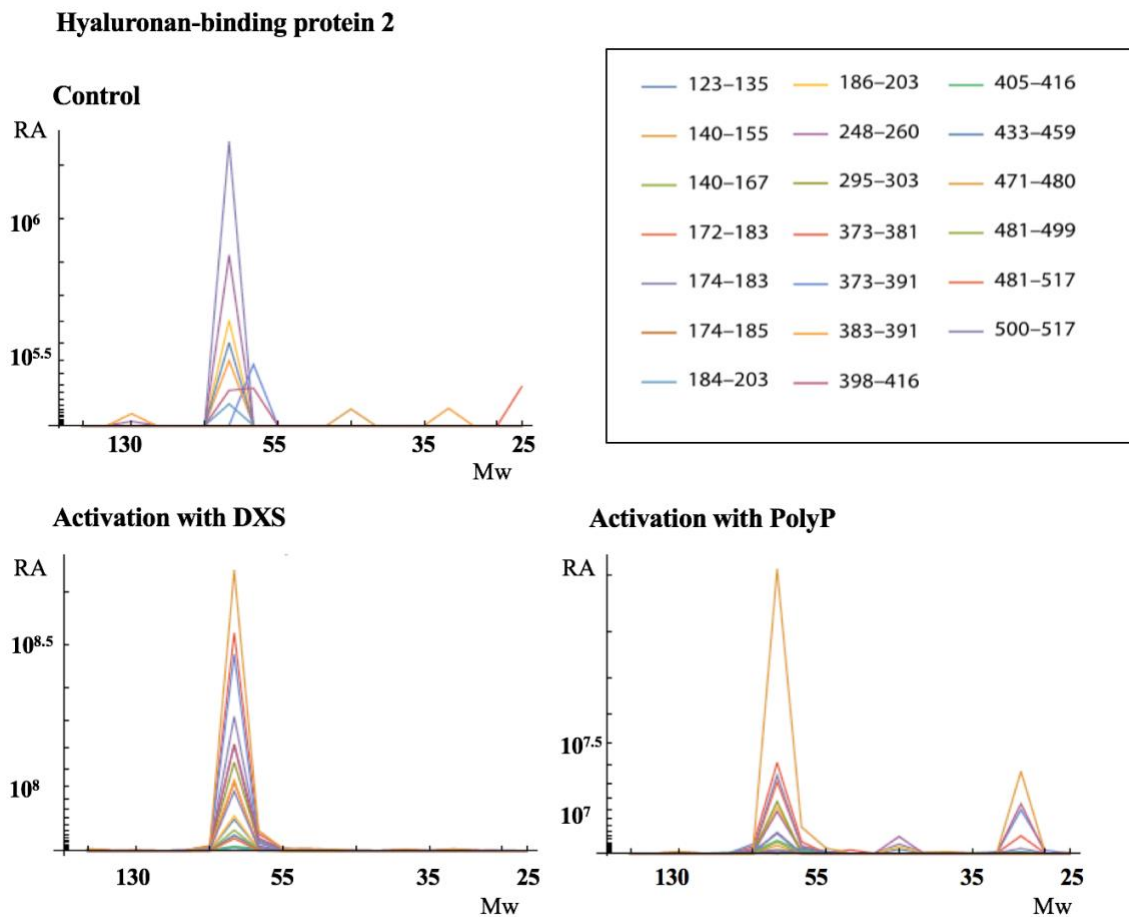**Figure 22:** Migration profile of the identified Hyaluronan-binding protein 2 (HABP2) species. HABP2 was identified by 20 peptides. The relative abundance (RA, in a.u.) of each peptide is plotted against the empirical molecular weight (Mw, in kDa). Each colored line represents a different tryptic peptide (amino acid positions shown in the legend – top right). After activation the overall relative amount of Hyaluronan-binding protein 2

Alpha-2-antiplasmin

Alpha-2-antiplasmin (α2AP) is a serine protease inhibitor that specifically targets plasmin, trypsin and chymotrypsin[57]. The migration profiles of α2AP show that its relative abundance is increased upon incubation of plasma with DXS and PolyP (figure 23). All identified peptides of the control sample are concentrated in the 60 kDa band that corresponds to the intact species of the protein. A shift towards the band containing FXII (80 kDa) is noticeable in both samples that had been incubated with the FXII activators, suggesting a possible interaction with FXII. A signal indicating a α 2AP with a higher molecular weight is visible in the control sample and in the DXS-activated sample.

Figure 23: Migration profiles of the identified Alpha-2-antiplasmin (α2AP) species identified by 7 peptides. The relative abundance (RA, in a.u.) of each peptide is plotted against the empirical molecular weight (Mw, in kDa). Each colored line represents a different tryptic peptide (amino acid positions shown in the legend – top right). The overall relative abundance of the protein is higher in both activated samples.

Alpha-2-Macroglobulin

Alpha-2-Macroglobulin is a universal protease inhibitor which is able to inhibit proteases from all classes[60]. This protein was found in its intact form (> 160 kDa) with similar relative abundance in all three samples and does not present major shifts in the migration profiles (figure 24). The bait region (P690-T728) including the three protease specific substrate domains (R704-E709, R719-H723 and T730-F735) was identified in all three samples.
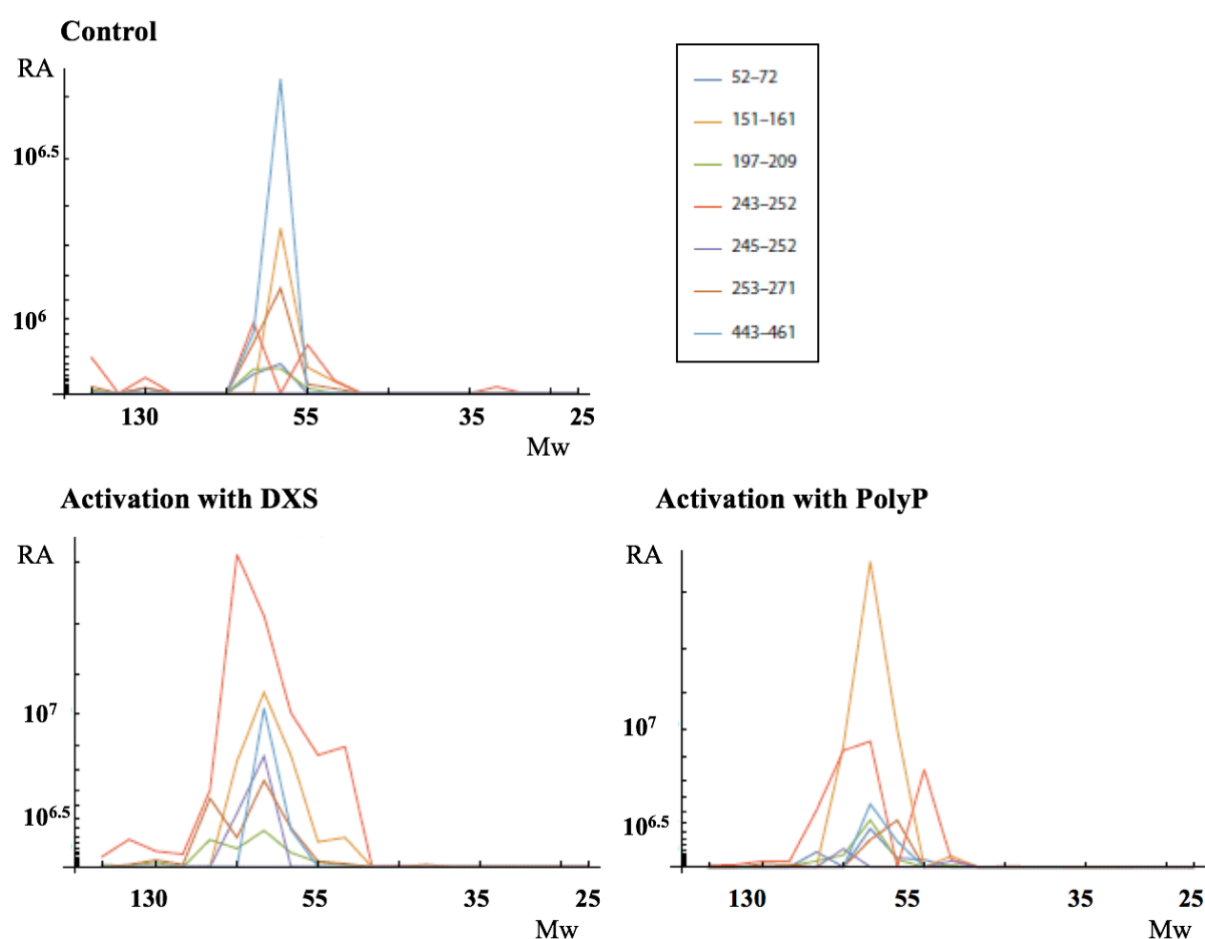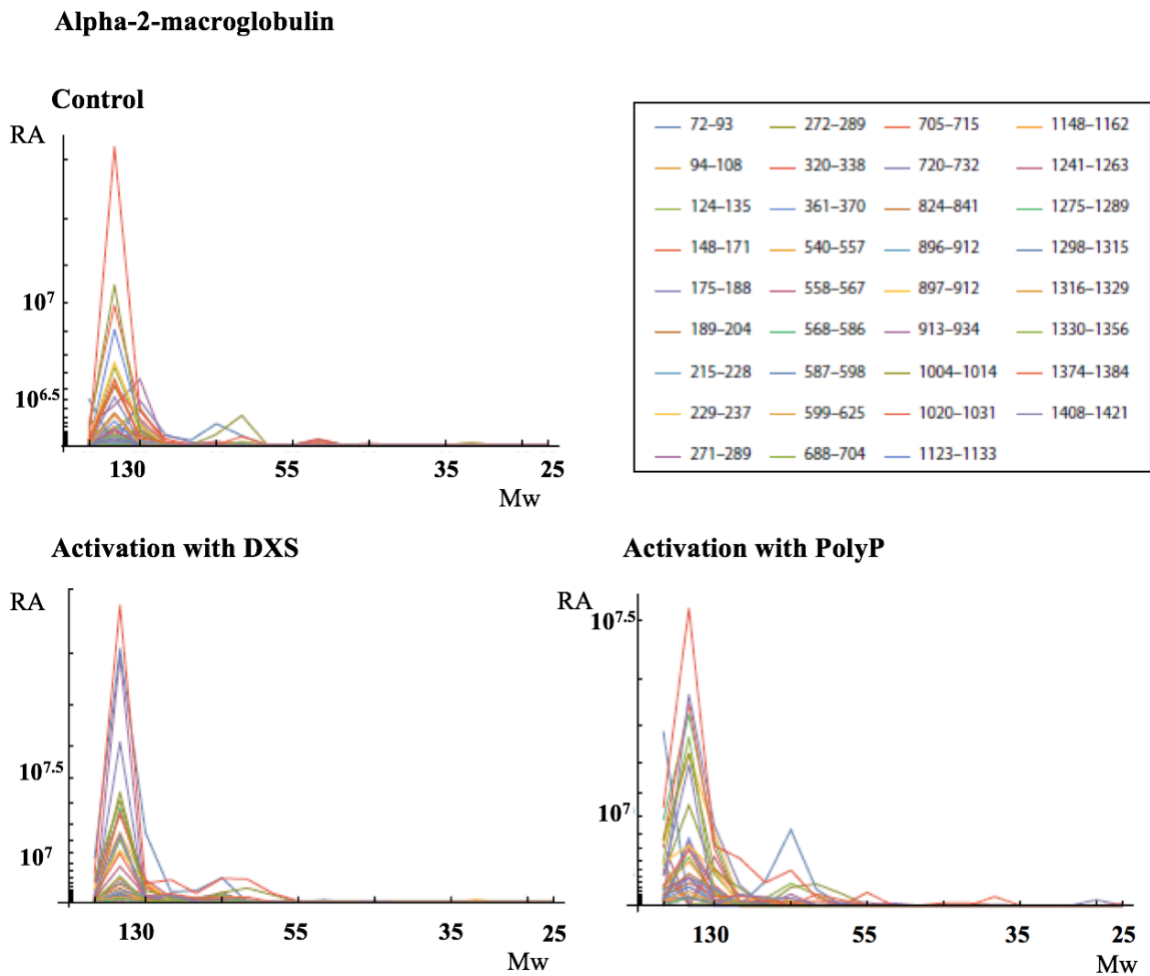

Figure 24: Migration profile of the identified Alpha-2-Macroglobulin species identified by 35 peptides. The relative abundance (RA, in a.u.) of each peptide is plotted against the empirical molecular weight (Mw, in kDa). Each colored line represents a different tryptic peptide (amino acid positions shown in the legend – top right). The overall relative abundance of the protein is higher in both activated samples. All identified peptides of the control sample are concentrated in the 60 kDa band that corresponds to the intact protein. A shift towards the band containing FXII (80 kDa) is noticeable in both activated samples and is more intense in the sample activated with DXS.

This protease inhibitor has also been described as an inhibitor for FXIIa but does not seem to be affected in dependence of the FXII activating molecule.

Inter-alpha-trypsin inhibitor heavy chain H4

Inter-alpha-trypsin inhibitor heavy chain H4 (ITIH4) is an acute-phase protein involved in inflammatory responses to trauma and is reported to inhibit endopeptidase activity[61]. During the analysis of all obtained migration profiles this protein stood out due to a significant increase of a ITIH4 protein species with 90 kDa. After the immunoaffinity enrichment for active FXII the overall relative abundance of this protein increased in the plasma samples incubated with DXS and PolyP (figure 25), suggesting an interaction of ITIH4 with FXIIa. Also, a shift of all identified peptides towards the FXII band is noticeable in the incubated samples, whereas in the control sample all identified peptides remain in a single confined band that corresponds to the intact protein. In both activated samples the majority of the peptides were found with great intensity in the band corresponding to 90 kDa. Nevertheless, differences can be found in the migration profiles of the sample incubated with DXS and PolyP. After activation of FXII with DXS besides the Intact ITIH4 (130 kDa) presenting a much lower relative abundance, the appearance of a species in the 30 kDa band was visible, suggesting proteolytic processing of the protein. In comparison with the sample incubated with PolyP the relative abundance species with 130 kDa band remained higher, and the species at 30 kDa was not present.
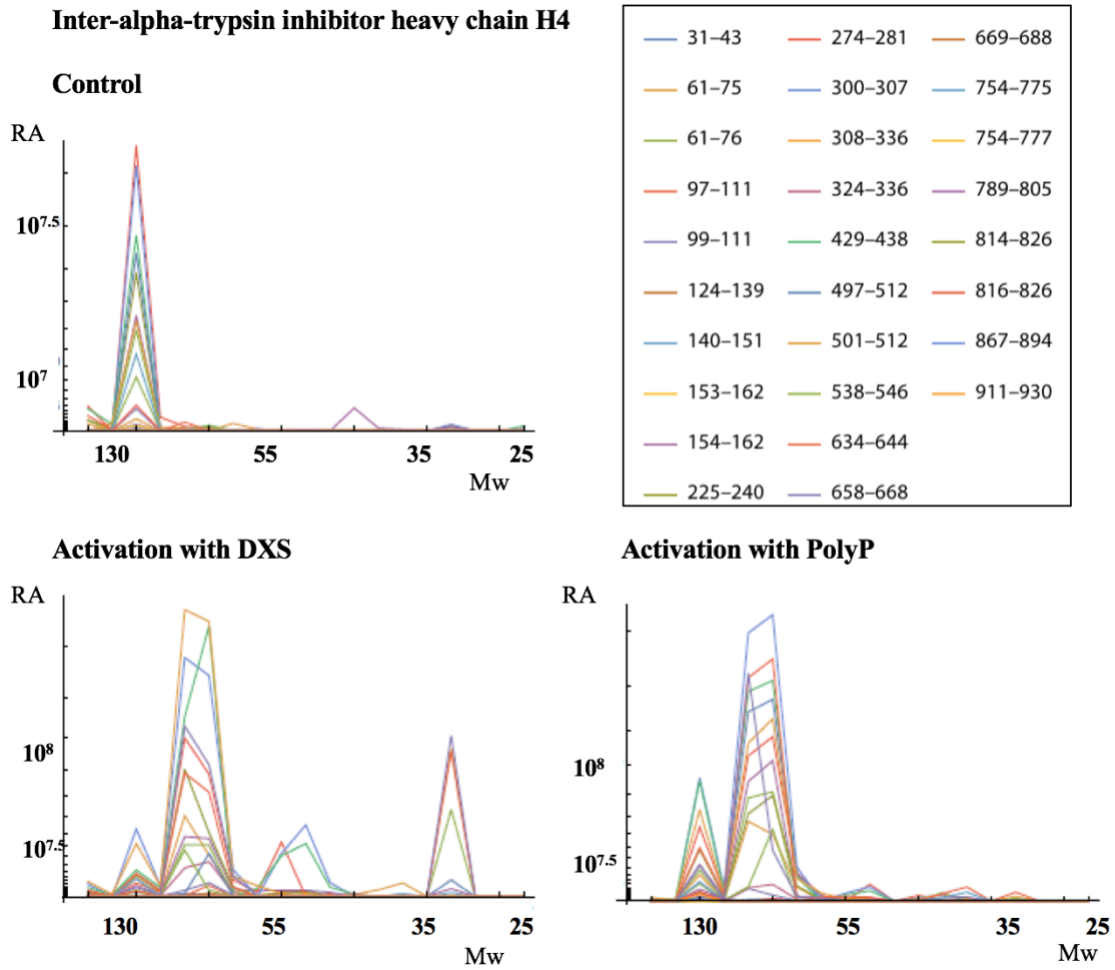
Figure 25: Migration profile of the identified Inter-alpha-trypsin inhibitor heavy chain H4 (ITIH4) species identified by 28 peptides. The relative abundance (RA, in a.u.) of each peptide is plotted against the empirical molecular weight (Mw, in kDa). Each colored line represents a different tryptic peptide (amino acid positions shown in the legend – top right). In the control sample all identified peptides are confined to the 130 kDa band and above. After activation with DXS and PolyP most peptides are found with great intensity at 90 kDa. Activation with DXS results in the generation of a 30 kDa fragment contrary to activation with PolyP, where in comparison the intact species is more abundant.

Discussion

Different activation mechanisms of the contact system and its biological relevance

Non-physiological compounds such as the polysaccharide dextran sulfate (DXS) [33,34] are well described sources of negative charges able to activate factor XII (FXII) *in-vitro*. Endogenous molecules such as platelet released Polyphosphate (PolyP)[62,63] have been shown to activate FXII *in-vivo*. Therefore, these compounds are regularly used as activators of the contact system for diagnostic or research purposes. While both substances induce an inflammatory response, only PolyP leads to coagulation[35]. It is therefore, hypothesized that:

> *The mechanism of activation of factor XII differs in the presence of by PolyP and DXS.*

This work aims to decipher the activation mechanism of FXII, analyzing the response of downstream proteins to contact system activation with respect to inflammation, coagulation, fibrinolysis and inhibition.

For many years the biological function of inorganic phosphate polymers was unclear. In humans, the presence of these polymers was first verified in acidocalcisome like structures in platelets, the dense granules[64]. Upon platelet activation, the content of the dense granules is released and the PolyP forms aggregates on the platelets surface to promote FXII activation[65] to promote coagulation. In contrast, DXS is an exogenous activator of the contact system regularly used in research of the contact system. Dextrans are produced by bacteria, such as Leuconostoc, Lactobacillus and Streptococcus. The dextrans are used as an extracellular biofilm to evade the immune system, for example evading fagocytosis[66]. The inflammatory pathway is initiated by the autoactivation of FXII and ultimately results in the release of bradykinin (BK). In case of an immunological response towards a bacterial infection, this pathway can be activated by the biofilm of dextrans. The use of DXS to induce colitis – inflammatory

bowel disease – in mice demonstrates its power to produce symptoms of inflammation[67]. Hence, the incubation of plasma with DXS is expected to trigger the pathway of inflammation.

To understand the underlying mechanisms of action of the activator molecules and their consequences on the contact system the obtained migration profiles were used to identify the protein species that were formed after plasma had been differentially incubated with PolyP and DXS.

From the results obtained in this work the activation of the inflammatory pathway by DXS is evident. As shown in figure 20 B, the proteolytic processing of FXII after incubation with DXS has occurred, noticeable by the appearance of the active FXII (FXIIa) species at lower molecular weights. Analyzing the obtained migration profiles with respect to the FXII heavy and light chain resulted from proteolytic cleavage (figure 19) a clear separation of both chains was detected. In comparison, these species do not appear in the control plasma (figure 19), and are of low relative abundance in the plasma activated with PolyP (figure 19). With the sole comparison of the FXII migration profiles one could assume that incubation of plasma with PolyP does not result in FXII activation. Therefore, the proteins downstream in the kallikrein-kinin system were analyzed. Plasma pre-kallikrein (PPK) circulates as an 85 kDa zymogen and is proteolytically activated by FXII, resulting in a lower molecular weight species plasma kallikrein (PK)[68]. In figures 20 B and 20 C, the proteolytic activation of PK was confirmed by the decrease of the relative abundance of the 80 kDa species and the increase of the smaller 40 kDa protein species when compared to the control (figure 20 A). These findings suggest that even though intact single chain FXII is the predominant species in the presence of PolyP it is still able to convert PPK to PK by proteolytic cleavage. Furthermore, the release of bradykinin (BK) from high molecular weight kininogen (HK) proves the activation of the kallikrein-kinin system[69] and was shown by the complete conversion of HK (130 kDa) into the two 55 kDa chain molecule. This conversion was demonstrated in the migration profiles of HK in figure X by the disappearance of the signal at 130 kDa in the activated plasma samples in comparison to the control. It is

arguable that the two chain HK species was also present in a relatively high amount in the control, represented by the signal in the bands slightly above 55 kDa (figure 20 A). This species can be explained by the presence of low-molecular weight kininogen (LK), an alternative splicing form of the KNG1 gene [70]. The amino acid sequence of LK is identical to HK until residue 384, after which V402-S626 is exchanged for SHLRSCEYKGRPPKAGAEPASEREVS. LK is much shorter, being only 409 aa long instead of 626 and has therefore, an empirical molecular weight of about 68 kDa[71]. Using the migration profiles of human serum albumin (65 kDa) in figure18 as a reference, it can be inferred that the signal above 55 kDa corresponded to the intact LK and not to processed HK.

From the obtained results, it can be stipulated that the FXII-mediated kallikrein-kinin system activation occurs when plasma comes into contact with any of the two molecules: DXS and PolyP. These findings are in accordance with Engel et al. describing that single chain FXII demonstrates proteolytic activity when incubated with PolyP. In contrast, incubation of plasma with DXS always resulted in proteolytic activation of FXII and formation of the FXIIa species[56]. It is assumed that the conformational change of FXII induced by DXS results in the auto-proteolytic cleavage of the R353-V354 bond to produce the two chain FXIIa. The conformational change induced by PolyP, however, does not promote auto-proteolysis, producing a proteolytically active single chain FXII species.

Knowing that the mechanism of activation results in different active FXII species, it can be further hypothesized that:

> *The substrate specificity of the active single chain FXII differs from that of proteolytically activated FXII.*

To test this hypothesis, the obtained results were screened for different protein species generated in plasma upon incubation with PolyP and DXS.

One of these proteins is hyaluronan-binding protein 2 (HABP2), a glycosaminoglycan binding plasma serine protease which consists of an N-terminal region (NTR), three

epidermal growth factor (EGF)-like domains, a Kringle domain and a serine protease domain[72]. The protein is synthesized as a single chain inactive zymogen (pro-HABP2) and undergoes autoproteolytic cleavage to form the active heterodimer[73]. The migration profiles obtained for HABP2 have shown an increase of its relative abundance in the plasma samples after incubation with DXS and PolyP (figure 22), meaning that once the FXII contact system is activated this protein interacts with FXIIa. This interaction might be mediated by the negative charges of the activating molecules that provide a common surface, interacting with HABP2 and FXII at the same time. Apart from the increase of relative abundance being higher in the plasma sample incubated with PolyP, the migration profile of HABP2 showed differences in comparison to the migration profile of HABP2 in plasma incubated with DXS. Upon FXII activation by PolyP, additional lower molecular weight species of HABP2 were identified in bands corresponding to 30 and 50 kDa demonstrating proteolytic cleavage of HABP2. When HABP2 undergoes proteolytic cleavage at G23 or M27 and cleavage at R313 or K319 it results in two new protein species consisting of one 50 kDa heavy chain and a 27 kDa light chain[72]. Polyamines have been described to favor the intramolecular NTR-E3 interaction that consequently allows intermolecular binding between NTR and E3 from another pro-HABP2 molecule forming an autoactivation complex[73]. Contrary to the contact system which is activated by negatively charged surfaces, polyamines are positively charged molecules. Nevertheless, several studies on HABP2 activation have shown that pro-HABP2 binds to polyanionic surfaces[74–77] via EGF3 domain that contains a cluster of positively charged amino acids. Depending on their size and charge density, binding to these negatively charged molecules results in cleavage of pro-HABP2 into its active species. PolyP is able to activate HABP2 in dependence of the chain length. The active species of HABP2 is then able to proteolytically activate several enzymes including factor VII (FVII), therefore activating coagulation[44]. In this work activation of HABP2 was shown by the appearance of the lower molecular weight species in the sample that had been incubated with PolyP. The sample incubated with DXS did not show proteolytic cleavage, hence no activation of HABP2. Muhl et al. have shown that in the presence of anticoagulants, such as small

heparin derivates and heparan sulfate, HABP2 is not proteolytically activated. In this work, the proteolytic activation of HABP2 was also not observed in the presence of DXS. It is concluded that in the presence of PolyP, HABP2 is proteolytically activated promoting coagulation via FVII and the extrinsic pathway of coagulation. In the presence of DXS however, HABP2 is not proteolytically activated and hence not able to activate coagulation.

Another protein of interest in regard to coagulation is antithrombin III (ATIII), a known FXII inhibitor. ATIII is a serpin targeting proteases of the contact activation pathway[78,79]. Analogously to the C1-inh, ATIII inhibits serine proteases by targeting the active serine in the catalytic triad with the reactive bond R393-S394 and covalently binding to it. The relative abundance of ATIII increased in both incubated plasma samples, confirming that ATIII interacts with FXII. The mechanism of this interaction seems to differ whereas the activation of FXII is induced via DXS or via PolyP (figure 21). This is shown by the appearance of an ATIII species at higher molecular weights upon incubation with DXS. Specially the ATIII species identified by the unique peptide ATEDEGSEQKIPEATNR (62-79) showed a significant shift towards the band containing FXII. This ATII species contains the N-terminal heparin binding domain[80,81]. Several mutations within the heparin binding domain of ATIII have been described to be responsible for a lack of heparin binding properties. When high molecular weight heparin (15 kDa) binds to ATIII, it facilitates the binding to active factor X (FXa) and thrombin and therefore, potentiating its anticoagulation activity[82]. Low molecular weight heparin (5 kDa) and polysaccharides such as Fondaparinux and DXS are too small to simultaneously bind to ATIII and thrombin, therefore only enhancing the ATIII capacity to bind to FXI and inhibiting coagulation[83]. The capacity of DXS to enhance the inhibitory effect of ATIII towards FXI provides an explanation for the lack of coagulation although FXII has been activated in the presence of DXS. The observed shift in the migration profile of ATIII towards the molecular weight of FXII, FXI and higher molecular weights is indicative of a covalent binding to proteases of the coagulation pathway and thereby promoting their inhibition.

DXS provides a negatively charged surface which induces the auto-cleavage of FXII zymogen, activating the downstream proteolytic cascade of the contact system. DXS binds to ATIII, potentiating its inhibitory activity towards the coagulation pathway. Hence, promoting the release of bradykinin by activation of the inflammatory pathway without the occurrence of coagulation.

Muhl et al, has shown that heparan sulfate and heparin serve as co-factors for ATIII in the inhibition of HABP2 and that the HABP2 activity was increased in the presence of low-molecular-weight heparin and PolyP even in the presence of ATIII[44]. These findings also support the hypothesis that the coagulation pathway is inhibited in the presence of DXS. The here proposed molecular mechanisms with respect to coagulations are summarized in figure 26.
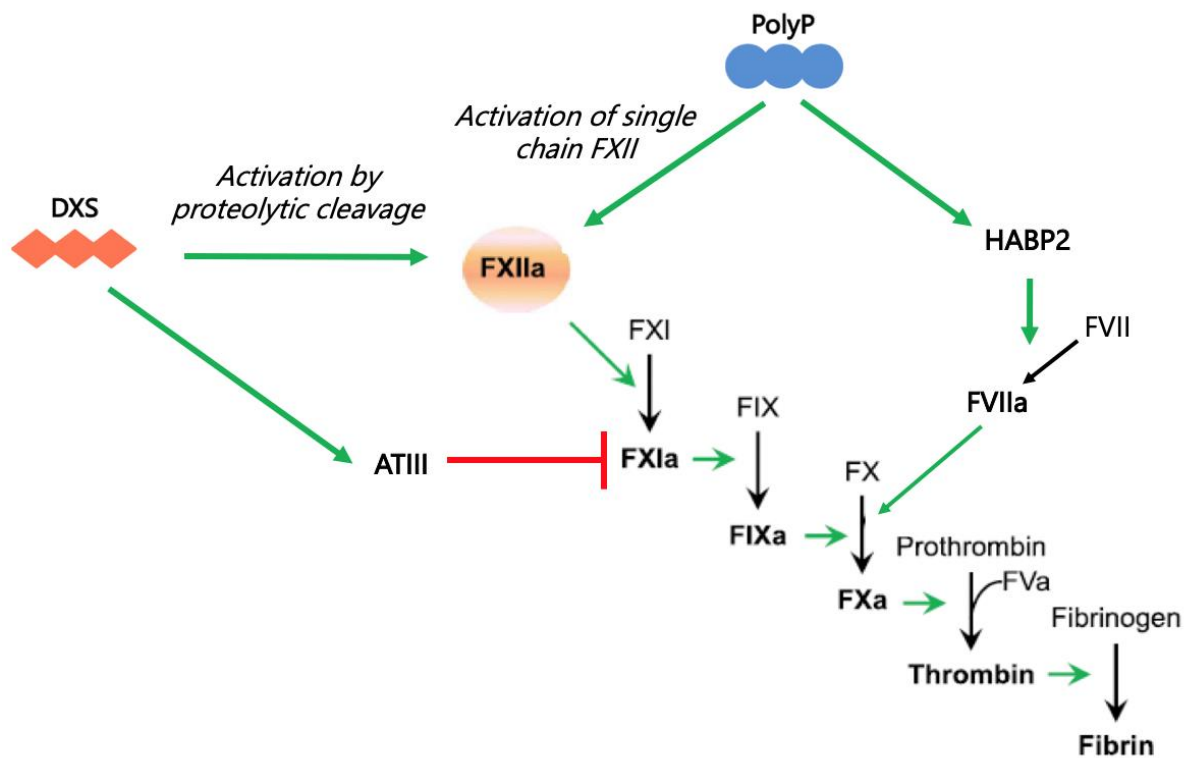
Figure 26: Effect of dextran sulfate (DXS) and Polyphosphate (PolyP) on the coagulation pathway. Green arrows represent activation. Inhibition is represented by red lines. Black arrows represent conversion from inactive to active protein species. Dextran sulfate aids in the recruitment of antithrombin III (ATIII) to inhibit the active coagulation factor XI (FXIa) inhibiting coagulation. PolyP activates hyaluronan-binding protein 2 (HABP2 that promotes he activation of factor FVII via the extrinsic pathway of coagulation and therefore potentiating coagulation.

In order to maintain homeostasis, fibrinolysis, the proteolytic cascade that results in the degradation of fibrin polymers from blood clots, is activated. Activated endothelial cells close to the blood clot release tissue-type plasminogen activator (tPA). This structural homologue of FXII, binds to the clot and converts plasminogen into the active form, plasmin, the main serine protease responsible for clot dissolution[84]. Fibrinolysis is also activated by PK driven urokinase-type plasminogen activator (uPA) that forms plasmin from plasminogen by proteolysis[85]. After plasmin dissociates from the clot, it is irreversibly inactivated by alpha-2-antiplasmin (α2AP).

α2AP belongs to the serpin family of protease inhibitors. Along with trypsin, plasmin belongs to the major targets of this 70 kDa serine protease inhibitor. α2AP circulates as a zymogen and is activated by antiplasmin-cleaving enzyme (APCE) upon cleavage of the P39-N40 peptide bond converting Met-α2AP into Asn-α2AP[86,87]. The obtained results have shown an increase in relative abundance of α2AP in the interactome of FXIIa suggesting its recruitment upon incubation of plasma with any of the two FXII activating molecules. This is in coherence with the activation of uPA by PK upon contact activation of FXII. Although this serpin is highly abundant in plasma (70 µg/ml), the N-terminus was not identified in any of the samples, meaning that in the obtained results the active species could not be distinguished from the zymogen. Nevertheless, the active form is more likely to be crosslinked to fibrin from the blood clot, resulting in a α2AP-Fibrin species with 130 kDa and larger[86]. This species was identified in the control sample and in the sample incubated with DXS (figure 23). Both species of α2AP have been described to inhibit FXIIa and tPA[88]. The obtained results in this work show that upon DXS activation of FXII, a α2AP-species with a higher molecular weight is formed.

HABP2 has also been described to cleave single chain urokinase activators (scu-PA)[44,89,90] with a comparable efficiency of established scu-PA activators[91] as well as the alpha chain of fibrinogen, being therefore, indirectly involved in fibrinolysis. This serine protease was heavily enriched after incubation with any one of the two activators (Figure 22). Cleavage of HABP2 to produce the its active species was observed in the

plasma sample upon incubation with PolyP but not in the presence of DXS. Nevertheless, the high relative abundance of HABP2 in the samples incubated with DXS in comparison to the control suggests that DXS provides the negative surface to aid in the recruitment of HABP2, possibly aiding in the fibrinolytic pathway. Hereby it can be concluded that the fibrinolytic pathway is promoted in the presence of both FXII activating molecules, either in the recruitment or in the direct activation of proteases, by DXS and PolyP, respectively.

Recent findings suggest that the current paradigm of the negatively charged surfaces for activation of the contact system needs a revision. Vogler et al. have demonstrated that not only the negatively charged surfaces are able to induce contact system activation, but it is also substantially influenced by the protein composition in the fluid. They postulate that the underlying mechanism that triggers FXII activation is a conformational change due to denaturation[92]. Gebbnick et al. have found that protein aggregates resulting from misfolding or partial denaturation can induce FXII contact activation[93]. These findings are also in accordance with the findings in this work, where FXII activity did not seem to be dependent on proteolytical cleavage.

Mechanisms of FXII inhibition

Since the discovery that FXII deficient individuals don't suffer from abnormal bleeding and are protected against thrombosis, FXII has become an interesting target for the development of antithrombotic drugs[94,95]. Understanding FXII inhibition is therefore the key in finding alternative therapies for thrombosis.

The migration profile assay was used to unravel the mechanisms underlying FXII inhibition. Therefore, the known inhibitors for FXII were analyzed. The extensively described and best-known inhibitor of FXII is the C1-inhibitor (C1-inh). C1-inh is a serine protease inhibitor that offers the R445 residue as a substrate to the reactive serine of FXII. FXII cleaves the R445 – T446 bond of the C1-inh. The cleavage is followed by a rapid conformational change of C1-inh, so that the cleavage product of C1-inh can no longer leave the catalytic pocket of FXII and remains covalently bound to the

light chain of FXII. C1-inh is therefore called a suicide inhibitor. The formation of the covalent bond between FXIIa and C1-inh constitutes a protein species with a molecular weight of about 130 kDa (composed of the 28 kDa FXIIa-light chain and 100 kDa C1-inh). This 130 kDa fusion protein was identified by the appearance of a signal at 130 kDa in the migration profile of FXII after its activation by any of the two activator molecules used (figure 20 B and C). The FXIIa-C1-inh fusion protein was also identified in the migration profiles from both proteins (FXII in figure 14 and C1-inh in figure 15) in the bands corresponding to 130 kDa after the incubation of plasma with the FXII activator DXS. The co-localization of C1-inh and FXII in bands corresponding to higher molecular weights was therefore evidence for the covalent binding between these proteins. Ultimate confirmation of the newly formed protein species would have been the identification of the covalently bound tryptic peptides containing the reactive residues from both proteins (figure 16), but this molecule could not be identified in any of the experiments. The database-driven protein identification relies on the produced fragment spectra of single peptides[18]. Fragmentation of two covalently bound tryptic peptides would have resulted in a complex fragment spectrum not identifiable with conventional database search. Furthermore, the full-scan spectra were acquired in a range of 400 to 1600 m/z. The 9934.57 Da molecule of the two covalently bound peptides would have had to be seven-fold charged, resulting in a signal at m/z 1420.22, to be detectable within the acquired m/z range. Manual search for the 1420.22 m/z precursor did not yield any results. According to the amino acid composition of the covalently bound peptides, the theoretical charge of the molecule at pH 2.3 would be +5[55]. The five times charged molecule has an m/z value of 1987.91, which is outside the set m/z range. Furthermore, the size and hydrophobicity of the fused peptide could result in an irreversible binding to the C18 material of the reversed phase column, so the fusion peptide would not reach the mass spectrometer at all.

Alpha-2-Macroglobulin (α2M) is a universal protease inhibitor able to inhibit all four classes of proteases. At a normal concentration of 1.2 mg/ml, α2M circulates abundantly in the plasma as a tetramer[96]. The obtained results in this thesis show a

relatively high abundance of the intact monomer in all samples (figure 24). Unlike the serpins, α2M inhibits the target proteases by a trapping mechanism. The bait region, located between the residues P690-T728, targets and binds to the proteases[97]. After the baited protease cleaves a peptide bond from the bait region, α2M undergoes a conformational change and a hydrolyzed thioester bond mediates covalent binding of the baited protease to α2M building a cage-like structure around the target protease[98]. Due to the steric hindrance, the encaged protease's activity against lager target molecules is greatly reduced but is still remains active in the cleavage of lower molecular weight molecules. Therefore, once α2M is covalently bound to its substrate the appearance of a higher molecular weight species of α2M would be expected. Since α2M is already a 180 kDa protein, the new protein species composed of α2M and the bound protease will larger than 200 kDa and thus not represented in the acquired migration profiles. For an adequate understanding of the involvement of α2M in the contact system, the assay would have to be applied with a different SDS gel to resolve species with molecular weights higher than 200 kDa.

The presented endogenous inhibitors for FXIIa, PK and FXIa greatly differ in potency towards their target proteases. For example, the inhibition efficacy of FXIIa by C1INH is over 150 times higher than by ATIII and α2M[88].

Aiming for the discovery of undescribed mechanisms of FXII inhibition, the obtained migration profiles were searched for alterations after the plasma has been incubated with the activating molecules. The alterations in the migration profile of inter-alpha-trypsin inhibitor heavy chain H4 (ITIH4) were apparent (figure 25). Apart from an increased relative abundance of ITIH4 after incubation of FXII with PolyP and DXS, indicating that its interaction with FXII is potentiated by any of the two molecules, appearance of new protein species at 90 kDa can be appreciated. ITIH4 is secreted by the liver into the bloodstream and is part of a protein-glycosaminoglycan-protein (PGP) complex, the inter-alpha-trypsin inhibitor (IαI) family. The PGP complex is composed of one or two of four heavy chains (ITIH1-ITIH4) covalently bound to the chondroitin sulfate chain of the light chain named bikunin[99,100] which carries the actual

inhibitory function. ITIH4 undergoes proteolytical cleavage by PK prior to binding to the chondroitin sulfate of bikunin[101]. After cleavage of ITIH4 into a 100 kDa and a 35 kDa species, the 100 kDa species is further converted into a 70 kDa species. As shown in figure 25, ITIH4 underwent proteolytical cleavage in the presence of PolyP and DXS. Interestingly, in the presence of DXS the smaller species of ITIH4 was formed, that was not present in the sample incubated with PolyP. The PGP complex has been extensively described as a protease inhibitor for trypsin, chymotrypsin, plasmin[102] and neutrophil elastase[103] but none of these have been defined as the physiological target. The high plasma concentrations of over 150 µg/ml are not enough to compensate for the high Ki, being therefore only responsible for 5% of the inhibitory activity of plasma proteases[104]. It was proposed that IαI functions as a shuttle that facilitates the contact of proteases with their physiological inhibitor by trapping them[105]. Nevertheless, bikunin has been described to have increased activity against tumor cell bound plasmin when compared to soluble plasmin[106]. The half-life of bikunin is greatly prolonged when bound to IαI chains, increasing from 4 minutes to several hours, suggesting that the IαI chains have a protective function for bikunin.

Therefore, the results in this work support that ITIH4 is proteolytically cleaved when plasma is incubated with DXS or PolyP. The activation of the contact system and consequent activation of PK is the plausible cause for the proteolytic cleavage of ITIH4. Literature research revealed that ITIH4 cannot act alone as protease inhibitor, being part of a larger PGP complex including bikunin which carries the actual inhibitory activity. 90% of bikunin, however, circulates in blood bound to proteins of the inter-alpha-trypsin inhibitor family. It can be postulated that in the case of contact system activation, ITIH4 is activated by PK to bind to bikunin and act as a chaperone to bring proteases and their corresponding inhibitors into close proximity, facilitating the inhibition of the proteolytic cascades.

In summary, the application of the migration profile assay on the FXII contact system activation revealed underlying mechanisms of FXII activation in dependence on the activator molecule. The conformational change of FXII in the presence of PolyP results

in its activation without the cleavage of the R372-V373 peptide bond, thereby influencing the substrate specificity towards downstream proteins. The resulting single chain FXII can activate pathways of inflammation and coagulation. In the presence of PolyP activation HABP2 occurs potentiating coagulation. In the presence of DXS, the radical conformational change of FXII leads to the auto-proteolytic cleavage of the R372-V373 bond. The specificity of the resulting two chain FXIIa towards downstream proteins is affected in a manner that ATIII is activated. Activation of this strong serine protease inhibitor results in the inhibition of the coagulation pathway. It is therefore, suggested that PolyP should be the molecule of choice in studies regarding FXII activation of the intrinsic coagulation cascade, since it best represents the endogenous conditions without interfering with coagulation.

Materials and reagents

Chemicals and reagents used in this work are presented in table X. The used instruments are specified in the table X.

Table 5: Materials and reagents used in this work with corresponding distributor.

Material / Reagent	Distributor
10% Bis-Tris Criterion XT Precast Gel	Bio-Rad, Hercules, USA
Acetonitrile (ACN) hyper grade for LC-MS	Merck, Darmstadt, Germany
Ammonium bicarbonate	Fluka, Honeywell, Charlotte, USA
Dextran sulfate (DXS)	Sigma-Aldrich, St. Louis, USA
Dithiothreitol (DTT)	Sigma-Aldrich, St. Louis, USA
EDTA s-monovette	Sarstedt, Nümbrecht, Germany
Formic acid (FA) for MS	Fluka, Honeywell, Charlotte, USA
Iodoacetamide (IAA)	Sigma-Aldrich, St. Louis, USA
Lämmli Buffer 2x	Bio-Rad, Hercules, USA
P Dulbecco's Phosphate Buffered Saline (PBS)	Merck, Darmstadt, Germany
Polyphosphate (PolyP)	BK Giulini GmbH, Ladenburg, Germany
See Blue Plus2 Pre-stained Protein Standard	Thermo Fisher Scientific, Bremen, Germany
Sequencing grade modified Trypsin	Promega, Mannheim, Germany
Water (LC-MS grade)	Merck, Darmstadt, Germany

Table 6: List of instrumentation used

Instruments	Distributor
Acclaim PepMap® RSLC, 75µmx500µm, C18, 2µm, 100Å,	Thermo Fisher scientific, Bremen, Germany
Acclaim PepMap® µ-precolumn, C18, 300 µm × 5 mm, 5 µm, 100 Å,	Thermo Fisher Scientific, Bremen, Germany
Dionex ultimate 3000 nano UPLC	Thermo Fisher scientific, Bremen, Germany
Fused-silica emitter I.D. 10 µm,	New Objective, Woburn, USA
nano-Acquity Peptide BEH analytical column; 130 Å, 1.7 m, 75 µm x 200 mm)	Waters, Manchester, UK
nano-ACQUITY UPLC	Waters, Manchester, UK
Orbitrap Fusion	Thermo Fisher scientific, Bremen, Germany
Orbitrap QExcactive	Thermo Fisher Scientific, Bremen, Germany
SeeBlue Plus2 Pre-stained Protein Standard	Thermo Fisher Scientific, Bremen, Germany
Symmetry C18 Trap Column; 100 Å, 5 µm, 180 µm x 20 mm	Waters, Manchester, UK

Methods

Blood collection and plasma generation

Fresh blood was obtained from healthy volunteers using a butterfly needle and an EDTA s-monovette. Plasma was obtained by centrifugation at 3000 x g for 10 minutes at 4°C. The obtained plasma from 3 volunteers was pooled.

Contact system activation

Pilot experiment

In this experiment the following solutions were used

DXS solution: 40 μg/mL dextran sulfate in PBS

Staining solution: 0,025% Coomassie blue dissolved in 50% Water, 40% Methanol and 10% acetic acid

Destaining solution: 50% Water, 40% Methanol and 10% acetic acid

100 μL of whole plasma were incubated adding 100 μL of DXS solution and incubated for 30 minutes at 37°C. At the same time 100 μL of plasma were incubated with PBS at 37°C as a control. The activation was stopped with a 1:1 (v/v) addition of hot 2x Lämmli buffer, followed by a 5 min denaturation at 95°C. Assuming the total protein concentration in human plasma is 30 μg/μl, 1 μl of the plasma Lämmli buffer mixture (15 μg of protein) was applied onto a 10 % SDS-PAGE gel. A 120 V voltage was applied to the SDS-PAGE for 5min, followed 80 min 140 V. The gel was covered in staining solution and incubated on a shaker for two hours, followed by destaining until protein bands were clearly distinguishable from the background.

Differential contact system activation

This part of the experiment was performed by Ellinor Kenne of the Karolinska Institute in Stockholm, Sweden.

200 μL of whole plasma were differentially incubated with either 200 μL of DXS (250μg/mL) or PolyP (250 μg/mL). As a control 200 μL of PBS were added to 200 μL of Plasma. The samples were incubated at 37°C for 90 minutes and agitated every 15 minutes.

For Immunoprecipitation, the samples were pre-cleared with protein G-sepharose beads and then incubated with anti-FXII antibody-coated protein G-sepharose beads for 60 min, at 4 degrees and under constant rotation. Unpacifically bound proteins were removed by washing with 3 times with PBS and centrifugation. Bound proteins were eluted and denatured at 95°C for 5 min.

The eluates were loaded onto a 10% SDS-PAGE and stained with Coomassie blue. The obtained SDS-PAGE sealed and shipped to UKE.

In-gel tryptic digestion

In this section the following buffers were used:

Ammonium bicarbonate buffer: 100 mM Ammonium bicarbonate at pH 8

DTT buffer: 10 mM dissolved in ammonium bicarbonate buffer

IAA buffer: 55 mM dissolved in ammonium bicarbonate buffer

Digestion solution: 8 ng/mL trypsin in 100 μM Ammonium bicarbonate at pH 8

Each lane from the SDS-page was cut into 19 separate bands as shown in figure 9 and transferred into a 1.5 mL tube. These bands were cut into 1 mm$_2$ pieces. The gel pieces were washed by 3 shrink-swell cycles. To shrink the gel pieces 100 μL of ACN were added and incubated on a shaker for 10 min. The gel pieces were swollen by a 10 min incubation with 100 μL of Ammonium bicarbonate buffer, on a shaker. Reduction of

the disulfide bonds was performed adding 50 µL DTT buffer onto the shrunken gel pieces and incubation for 20 min at 57°C. After shrinking, the cysteines were alkylated adding IAA buffer and incubation for 30 min in the dark at room temperature. For digestion, the gel pieces were covered with digestion buffer and incubated at 37°C, overnight. Tryptic peptides were extracted by 3, 30-minute-long, shrink-swell cycles. The supernatant was transferred into a new vial and evaporated to complete dryness using a vacuum-centrifuge.

LC-MS/MS analysis

Mobile phase A 0.1 % (v/v) FA in water

Mobile phase B: 0.1 % (v/v) FA in ACN

All samples were dissolved in 20 µL of mobile phase A and subjected to liquid chromatography coupled to mass spectrometry (LC-MS/MS) analysis as follows.

Pilot experiment

For these samples LC-MS/MS analysis was performed using with a nano-liquid ultra-pressure liquid chromatography (nano-UPLC) system (*nano*-ACQUITY, Waters, Manchester, UK) coupled via a *nano*-electrospray ionization-source (NSI) source to a tandem mass spectrometer (MS/MS) consisting of a quadrupole and an orbitrap mass analyzer (Q-Exactive). 1 µL of each sample were loaded onto a reversed-phase (RP) trapping column (Symmetry C18) and washed for 5 min, with 1 % buffer B for 5 min. The peptides were eluted onto a RP capillary column (BEH analytical column) and separated by a linear gradient from 3 to 35 % buffer B in 35 min at a constant flowrate of 250 nL/min. Eluting peptides were ionized and desorbed by ESI in the positive mode using a fused-silica emitter at a capillary voltage of 1800 V. Data dependent acquisition mode was used with the following parameters: MS spectra were acquired over a m/z range from 400 to 1,500, with a resolution of 70,000 FWHM at m/z 200. Maximum injection time was set to 120 ms for an AGC target of 1e6. For MS/MS analysis the top 12 signals were isolated in a 2 m/z window and fragmented with a normalized HCD

collision energy of 25%. Fragment spectra were recorded with a resolution of 17,500 FWHM at m/z 200 Maximum injection time was set to 50 ms for an AGC target 1e5.

Differential contact system activation:

The nano-UPLC used for these samples was a Dionex ultimate 3000 coupled to Fusion Tribrid quadrupole, orbitrap and ion-trap mass spectrometer (Orbitrap Fusion, Thermo Scientific, Bremen, Germany), via nano-electrospray ionization-source (NSI). 1 µl of each sample was loaded onto a trapping column (Acclaim µ-precolumn,) and washed with 3% buffer B for 5 min. Then the peptides were eluted onto a reversed phase capillary column (Acclaim RSLC) and separated through a gradient from 3 to 28% buffer B in 35 min and from 28 to 35% in 40 min, at a constant flow rate of 300 nl/min. Eluting peptides were ionized by NSI at a capillary voltage of 1800 V. The maximum injection time was 120 ms for an AGC target of 2e5. The m/z range at MS level was set from 400 to 1300 Da with a resolution of 120.000 FWHM at m/z 200 for data dependent acquisition performed in Top Speed mode. The most intense precursor ions with intensity greater than 1e4 were selected for fragmentation with a normalized HCD collision energy of 30 %. Fragment spectra were recorded with a maximum injection time of 60 ms for an AGC target of 5e5 in the ion trap.

Protein identification

LC–MS raw data were processed with MaxQuant algorithms (version 1.5.8.3)[18]. Protein identification was carried out with Andromeda against the human (Homo sapiens) (www.uniprot.org, downloaded on November 11th, 2014) and a contaminant database. The searches were performed using a precursor mass tolerance set to 10 ppm and fragment mass tolerance set to 10 ppm or 0,4 Da for analysis with the Q-Exactive and the Fusion, respectively. For peptide identification two missed cleavages were allowed. Carbamidomethylation on the cysteine was set as fixed modification and for variable modifications oxidation of the methionine and acetylation on protein N-Terminus. A maximum of 5 modifications per peptide were allowed.

Migration profiles

Protein identification via MaxQuant generates several text files (.txt) containing information about the identified proteins and peptides. The "peptides.txt" contains a list of every single identified peptide, the corresponding protein, it's location within the amino acid. sequence and the measured intensity (A.U.C. from the extracted ion chromatogram of the peptide ion). The intensity of each peptide was plotted against the empirical molecular weight determined in the SDS-PAGE. This procedure was done manually using Microsoft Office Excel for factor XII and. extended to all identified proteins with a Wolfram Mathematica script.

References

1.   Wasinger VC, Cordwell SJ, Cerpa-Poljak A, Yan JX, Gooley AA, Wilkins MR, Harris R, Duncan MW, Williams KL, H.-S. I. Progress with gene-product mapping of the Mollicutes: Mycoplasma genitalium. - PubMed - NCBI. *Electrophoresis* 1090–1904 (1955).

2.   Kahn, P. From genome to proteome: looking at a cell's proteins. *Science* **270**, 369–70 (1995).

3.   Aebersold, R. & Mann, M. Mass spectrometry-based proteomics. *Nature* **422**, 198–207 (2003).

4.   Karas, M. & Hillenkamp, F. Laser desorption ionization of proteins with molecular masses exceeding 10,000 daltons. *Anal. Chem.* **60**, 2299–301 (1988).

5.   Fenn, J. B., Mann, M., Meng, C. K., Wong, S. F. & Whitehouse, C. M. Electrospray ionization for mass spectrometry of large biomolecules. *Science* **246**, 64–71 (1989).

6.   Mayne, J. *et al.* Bottom-Up Proteomics (2013–2015): Keeping up in the Era of Systems Biology. *Anal. Chem.* **88**, 95–121 (2016).

7.   Iavarone, A. T. & Williams, E. R. Mechanism of charging and supercharging molecules in electrospray ionization. *J. Am. Chem. Soc.* **125**, 2319–27 (2003).

8.   Kebarle, P. & Verkerk, U. H. Electrospray: from ions in solution to ions in the gas phase, what we know now. *Mass Spectrom. Rev.* **28**, 898–917

9.   Konermann, L., Ahadi, E., Rodriguez, A. D. & Vahidi, S. Unraveling the mechanism of electrospray ionization. *Anal. Chem.* **85**, 2–9 (2013).

10. Metwally, H., Duez, Q. & Konermann, L. Chain Ejection Model for Electrospray Ionization of Unfolded Proteins: Evidence from Atomistic Simulations and Ion Mobility Spectrometry. *Anal. Chem.* **90**, 10069–10077 (2018).

11. Hogan, C. J., Carroll, J. A., Rohrs, H. W., Biswas, P. & Gross, M. L. Combined charged residue-field emission model of macromolecular electrospray ionization. *Anal. Chem.* **81**, 369–77 (2009).

12. Paul, W. & Steinwedel, H. Notizen: Ein neues Massenspektrometer ohne Magnetfeld. *Zeitschrift für Naturforsch. A* **8**, 448–450 (1953).

13. Paul Wolfgang, S. H. Verfahren zur Trennung bzw. zum getrennten Nachweis von Ionen verschiedener spezifischer Ladung. (1953).

14. Makarov. Electrostatic axially harmonic orbital trapping: a high-performance technique of mass analysis. *Anal. Chem.* **72**, 1156–62 (2000).

15. Eliuk, S. & Makarov, A. Evolution of Orbitrap Mass Spectrometry Instrumentation. *Annu. Rev. Anal. Chem.* **8**, 61–80 (2015).

16. Planet Orbitrap. Available at: planetorbitrap.com.

17. Mitchell Wells, J. & McLuckey, S. A. Collision-Induced Dissociation (CID) of Peptides and Proteins. in *Methods in enzymology* **402**, 148–185 (2005).

18. Tyanova, S., Temu, T. & Cox, J. The MaxQuant computational platform for mass spectrometry-based shotgun proteomics. *Nat. Protoc.* **11**, 2301–2319 (2016).

19. Aebersold, R. & Mann, M. Mass-spectrometric exploration of proteome structure and function. *Nature* **537**, 347–55 (2016).

20. National Diagnostics. Available at: www.nationaldiagnostics.com.

21. Summers, D. F., Maizel, J. V, Darnell, J. E., Darnell, J. E. & Jr. Evidence for virus-specific noncapsid proteins in poliovirus-infected HeLa cells. *Proc. Natl. Acad. Sci. U. S. A.* **54**, 505–13 (1965).

22. Smith, B. J. SDS Polyacrylamide Gel Electrophoresis of Proteins. in *Proteins* 41–56 (Humana Press, 1984). doi:10.1385/0-89603-062-8:41

23. Li, C., Tan, X. F., Lim, T. K., Lin, Q. & Gong, Z. Comprehensive and quantitative proteomic analyses of zebrafish plasma reveals conserved protein profiles between genders and between zebrafish and human. *Sci. Rep.* **6**, 24329 (2016).

24. Rawlings, N. D. *et al.* The MEROPS database of proteolytic enzymes, their substrates and inhibitors in 2017 and a comparison with peptidases in the PANTHER database. *Nucleic Acids Res.* **46**, D624–D632 (2018).

25. MEROPS peptidase database. Available at: https://www.ebi.ac.uk/merops/.

26. Travis, J. & Salvesen, G. S. Human plasma proteinase inhibitors. *Annu. Rev. Biochem.* **52**, 655–709 (1983).

27. Dodson, G. & Wlodawer, A. Catalytic triads and their relatives. *Trends Biochem. Sci.* **23**, 347–52 (1998).

28. Hedstrom, L. Serine protease mechanism and specificity. *Chem. Rev.* **102**, 4501–24 (2002).

29. Schmaier, A. H. Physiologic activities of the contact activation system. *Thromb. Res.* **133 Suppl 1**, S41-4 (2014).

30. Kheirabadi, B. S. *et al.* Safety evaluation of new hemostatic agents, smectite granules, and kaolin-coated gauze in a vascular injury wound model in swine. *J. Trauma* **68**, 269–78 (2010).

31. Wiggins, R. C. & Cochrane, C. C. The autoactivation of rabbit Hageman factor. *J. Exp. Med.* **150**, 1122–33 (1979).

32. Bock, P. E., Srinivasan, K. R. & Shore, J. D. Activation of intrinsic blood coagulation by ellagic acid: insoluble ellagic acid-metal ion complexes are the activating species. *Biochemistry* **20**, 7258–66 (1981).

33. Samuel, M., Pixley, R. A., Villanueva, M. A., Colman, R. W. & Villanueva, G. B. Human factor XII (Hageman factor) autoactivation by dextran sulfate. Circular dichroism, fluorescence, and ultraviolet difference spectroscopic studies. *J. Biol. Chem.* **267**, 19691–7 (1992).

34. Clarke, B. J. *et al.* Mapping of a putative surface-binding site of human coagulation factor XII. *J. Biol. Chem.* **264**, 11497–502 (1989).

35. Maas, C., Oschatz, C. & Renné, T. The plasma contact system 2.0. *Semin. Thromb. Hemost.* **37**, 375–81 (2011).

36. Naudin, C., Burillo, E., Blankenberg, S., Butler, L. & Renné, T. Factor XII Contact Activation. *Semin. Thromb. Hemost.* **43**, 814–826 (2017).

37. Weidmann, H. *et al.* The plasma contact system, a protease cascade at the nexus of inflammation, coagulation and immunity. *Biochim. Biophys. Acta - Mol. Cell Res.* **1864**, 2118–2127 (2017).

38. Renné, T., Schmaier, A. H., Nickel, K. F., Blombäck, M. & Maas, C. In vivo roles of factor XII. *Blood* **120**, 4296–4303 (2012).

39. Madeddu, P. *et al.* Role of the bradykinin B2 receptor in the maturation of blood pressure phenotype: lesson from transgenic and knockout mice. *Immunopharmacology* **44**, 9–13 (1999).

40. Renné, T., Dedio, J., David, G. & Müller-Esterl, W. High molecular weight kininogen utilizes heparan sulfate proteoglycans for accumulation on endothelial cells. *J. Biol. Chem.* **275**, 33688–96 (2000).

41. Lämmle, B. *et al.* Thromboembolism and bleeding tendency in congenital factor XII deficiency--a study on 74 subjects from 14 Swiss families. *Thromb. Haemost.* **65**, 117–21 (1991).

42. Maas, C. & Renné, T. Coagulation factor XII in thrombosis and inflammation. *Blood* **131**, 1903–1909 (2018).

43. Brown, M. R. W. & Kornberg, A. Inorganic polyphosphate in the origin and survival of species. *Proc. Natl. Acad. Sci.* **101**, 16085–16087 (2004).

44. Muhl, L. *et al.* High negative charge-to-size ratio in polyphosphates and heparin regulates factor VII-activating protease. *FEBS J.* **276**, 4828–39 (2009).

45. Bock, S. C. *et al.* Human C1 inhibitor: primary structure, cDNA cloning, and chromosomal localization. *Biochemistry* **25**, 4292–301 (1986).

46. Cicardi, M., Zingale, L., Zanichelli, A., Pappalardo, E. & Cicardi, B. C1 inhibitor: molecular and clinical aspects. *Springer Semin. Immunopathol.* **27**, 286–298 (2005).

47. Bork, K. Diagnosis and treatment of hereditary angioedema with normal C1 inhibitor. *Allergy Asthma. Clin. Immunol.* **6**, 15 (2010).

48. Perego, F. *et al.* Current and emerging biologics for the treatment of hereditary angioedema. *Expert Opin. Biol. Ther.* **19**, 517–526 (2019).

49. Wu, M. A., Zanichelli, A., Mansi, M. & Cicardi, M. Current treatment options for hereditary angioedema due to C1 inhibitor deficiency. *Expert Opin. Pharmacother.* **17**, 27–40 (2016).

50. Worm, M. *et al.* The factor XIIa blocking antibody 3F7: a safe anticoagulant with anti-inflammatory activities. *Allergy Eur. J. Allergy Clin. Immunol.* **3**, 247 (2015).

51. Bagot, C. N. & Arya, R. Virchow and his triad: a question of attribution. *Br. J. Haematol.* **143**, 180–190 (2008).

52. Iwaki, T., Cruz-Topete, D. & Castellino, F. J. A complete factor XII deficiency does not affect coagulopathy, inflammatory responses, and lethality, but attenuates early hypotension in endotoxemic mice. *J. Thromb. Haemost.* **6**, 1993–5 (2008).

53. Mackman, N. Triggers, targets and treatments for thrombosis. *Nature* **451**, 914–8 (2008).

54. Kwiatkowski, M. *et al.* Homogenization of tissues via picosecond-infrared laser (PIRL) ablation: Giving a closer view on the in-vivo composition of protein species as compared to mechanical homogenization. *J. Proteomics* **134**, 193–202 (2016).

55. Kwiatkowski, M. *et al.* Application of Displacement Chromatography to Online Two-Dimensional Liquid Chromatography Coupled to Tandem Mass Spectrometry Improves Peptide Separation Efficiency and Detectability for the Analysis of Complex Proteomes. *Anal. Chem.* **90**, 9951–9958 (2018).

56. Engel, R., Brain, C. M., Paget, J., Lionikiene, A. S. & Mutch, N. J. Single-chain factor XII exhibits activity when complexed to polyphosphate. *J. Thromb. Haemost.* **12**, 1513–22 (2014).

57. Szabo, R., Netzel-Arnett, S., Hobson, J. P., Antalis, T. M. & Bugge, T. H. Matriptase-3 is a novel phylogenetically preserved membrane-anchored serine protease with broad serpin reactivity. *Biochem. J.* **390**, 231–242 (2005).

58. Olsson, M. *et al.* Genome-wide analysis of genetic determinants of circulating factor VII-activating protease (FSAP) activity. *J. Thromb. Haemost.* **16**, 2024–2034 (2018).

59. Grasso, S. *et al.* Interaction of factor VII activating protease (FSAP) with neutrophil extracellular traps (NETs). *Thromb. Res.* **161**, 36–42 (2018).

60. Ambrus, G. *et al.* Natural Substrates and Inhibitors of Mannan-Binding Lectin-Associated Serine Protease-1 and -2: A Study on Recombinant Catalytic Fragments. *J. Immunol.* **170**, 1374–1382 (2003).

61. Albani, D., Balduyck, M., Mizon, C. & Mizon, J. Inter-α-inhibitor as marker for neutrophil proteinase activity: An in vitro investigation. *J. Lab. Clin. Med.* **130**, 339–347 (1997).

62. Müller, F. *et al.* Platelet polyphosphates are proinflammatory and procoagulant mediators in vivo. *Cell* **139**, 1143–56 (2009).

63. Smith, S. A. *et al.* Polyphosphate modulates blood coagulation and fibrinolysis. *Proc. Natl. Acad. Sci. U. S. A.* **103**, 903–8 (2006).

64. Ruiz, F. A., Lea, C. R., Oldfield, E. & Docampo, R. Human Platelet Dense Granules Contain Polyphosphate and Are Similar to Acidocalcisomes of Bacteria and Unicellular Eukaryotes. *J. Biol. Chem.* **279**, 44250–44257 (2004).

65. Weitz, J. I. & Fredenburgh, J. C. Platelet polyphosphate: the long and the short of it. *Blood* **129**, 1574–1575 (2017).

66. Meddens, M. J., Thompson, J., Leijh, P. C. & van Furth, R. Role of granulocytes in the induction of an experimental endocarditis with a dextran-producing Streptococcus sanguis and its dextran-negative mutant. *Br. J. Exp. Pathol.* **65**, 257–65 (1984).

67. Eichele, D. D. & Kharbanda, K. K. Dextran sodium sulfate colitis murine model: An indispensable tool for advancing our understanding of inflammatory bowel diseases pathogenesis. *World J. Gastroenterol.* **23**, 6016–6029 (2017).

68. Björkqvist, J., Jämsä, A. & Renné, T. Plasma kallikrein: The bradykinin-producing enzyme. *Thromb. Haemost.* **110**, 399–407 (2013).

69. Kaplan, A. P., Meier, H. L. & Mandle, R. J. The role of Hageman factor, prekallifrein, and high molecular weight kininogen in the generation of bradykinin and the initiation of coagulation and fibrinolysis. *Monogr. Allergy* **12**, 120–30 (1977).

70. Hosoi, K. *et al.* Expression of kininogens in the connective tissue-type mast cells of the rat. *Immunology* **101**, 531–40 (2000).

71. Ohkubo, I., Kurachi, K., Takasawa, T., Shiokawa, H. & Sasaki, M. Isolation of a human cDNA for alpha 2-thiol proteinase inhibitor and its identity with low molecular weight kininogen. *Biochemistry* **23**, 5691–7 (1984).

72. Choi-Miura, N. H. *et al.* Purification and characterization of a novel hyaluronan-binding protein (PHBP) from human plasma: it has three EGF, a kringle and a serine protease domain, similar to hepatocyte growth factor activator. *J. Biochem.* **119**, 1157–65 (1996).

73. Yamamichi, S., Nishitani, M., Nishimura, N., Matsushita, Y. & Hasumi, K. Polyamine-promoted autoactivation of plasma hyaluronan-binding protein. *J. Thromb. Haemost.* **8**, 559–66 (2010).

74. Etscheid, M., Hunfeld, A., König, H., Seitz, R. & Dodt, J. Activation of proPHBSP, the Zymogen of a Plasma Hyaluronan Binding Serine Protease, by an Intermolecular Autocatalytic Mechanism. *Biol. Chem.* **381**, 1223–31 (2000).

75. Kannemeier, C. *et al.* Factor VII and single-chain plasminogen activator-activating protease. *Eur. J. Biochem.* **268**, 3789–3796 (2001).

76. Altincicek, B. *et al.* A positively charged cluster in the epidermal growth factor-like domain of Factor VII-activating protease (FSAP) is essential for polyanion binding. *Biochem. J.* **394**, 687–692 (2006).

77. NAKAZAWA, F. *et al.* Extracellular RNA is a natural cofactor for the (auto-)activation of Factor VII-activating protease (FSAP). *Biochem. J.* **385**, 831–838 (2005).

78. YAMAMICHI, S., NISHITANI, M., NISHIMURA, N., MATSUSHITA, Y. & HASUMI, K. Polyamine-promoted autoactivation of plasma hyaluronan-binding protein. *J. Thromb. Haemost.* **8**, 559–566 (2010).

79. Lane, D. A., Olds, R. J. & Thein, S. L. Antithrombin III: summary of first database update. *Nucleic Acids Res.* **22**, 3556–9 (1994).

80. Muñoz, E. M. & Linhardt, R. J. Heparin-binding domains in vascular biology. *Arterioscler. Thromb. Vasc. Biol.* **24**, 1549–57 (2004).

81. Ersdal-Badju, E., Lu, A., Zuo, Y., Picard, V. & Bock, S. C. Identification of the antithrombin III heparin binding site. *J. Biol. Chem.* **272**, 19393–400 (1997).

82. Oschatz, C. *et al.* Mast cells increase vascular permeability by heparin-initiated bradykinin formation in vivo. *Immunity* **34**, 258–68 (2011).

83. Jaffer Iqbal, W. J. Antithrombotic Therapy. in (2014).

84. Rau, J. C., Beaulieu, L. M., Huntington, J. A. & Church, F. C. Serpins in thrombosis, hemostasis and fibrinolysis. *J. Thromb. Haemost.* **5 Suppl 1**, 102–15 (2007).

85. Lin, Y. *et al.* High molecular weight kininogen peptides inhibit the formation of kallikrein on endothelial cell surfaces and subsequent urokinase-dependent plasmin formation. *Blood* **90**, 690–7 (1997).

86. Lee, K. N., Jackson, K. W., Christiansen, V. J., Chung, K. H. & McKee, P. A. A novel plasma proteinase potentiates alpha2-antiplasmin inhibition of fibrin digestion. *Blood* **103**, 3783–8 (2004).

87. Christiansen, V. J., Jackson, K. W., Lee, K. N. & McKee, P. A. The effect of a single nucleotide polymorphism on human alpha 2-antiplasmin activity. *Blood* **109**, 5286–92 (2007).

88. Pixley, R. A., Schapira, M. & Colman, R. W. The regulation of human factor XIIa by plasma proteinase inhibitors. *J. Biol. Chem.* **260**, 1723–9 (1985).

89. Römisch, J., Vermöhlen, S., Feussner, A. & Stöhr, H. The FVII activating protease cleaves single-chain plasminogen activators. *Haemostasis* **29**, 292–9 (1999).

90. Stavenuiter, F. *et al.* Factor seven activating protease (FSAP): does it activate factor VII? *J. Thromb. Haemost.* **10**, 859–66 (2012).

91. Hoylaerts, M., Rijken, D. C., Lijnen, H. R. & Collen, D. Kinetics of the activation of plasminogen by human tissue plasminogen activator. Role of fibrin. *J. Biol. Chem.* **257**, 2912–9 (1982).

92. Vogler, E. A. & Siedlecki, C. A. Contact activation of blood-plasma coagulation. *Biomaterials* **30**, 1857–69 (2009).

93. Gebbink, M. F. B. G., Bouma, B., Maas, C. & Bouma, B. N. Physiological responses to protein aggregates: fibrinolysis, coagulation and inflammation (new roles for old factors). *FEBS Lett.* **583**, 2691–9 (2009).

94. Schmaier, A. H. & McCrae, K. R. The plasma kallikrein-kinin system: its evolution from contact activation. *J. Thromb. Haemost.* **5**, 2323–9 (2007).

95. Kenne, E. *et al.* Factor XII: a novel target for safe prevention of thrombosis and inflammation. *J. Intern. Med.* **278**, 571–85 (2015).

96. Coan, M. H. & Roberts, R. C. A redetermination of the concentration of alpha 2-macroglobulin in human plasma. *Biol. Chem. Hoppe. Seyler.* **370**, 673–6 (1989).

97. Doan, N. & Gettins, P. G. W. Human alpha2-macroglobulin is composed of multiple domains, as predicted by homology with complement component C3. *Biochem. J.* **407**, 23–30 (2007).

98. Andersen, G. R., Koch, T. J., Dolmer, K., Sottrup-Jensen, L. & Nyborg, J. Low Resolution X-ray Structure of Human Methylamine-treated α 2 -Macroglobulin. *J. Biol. Chem.* **270**, 25133–25141 (1995).

99. Enghild, J. J., Thøgersen, I. B., Pizzo, S. V & Salvesen, G. Analysis of inter-alpha-trypsin inhibitor and a novel trypsin inhibitor, pre-alpha-trypsin inhibitor, from human plasma. Polypeptide chain stoichiometry and assembly by glycan. *J. Biol. Chem.* **264**, 15975–81 (1989).

100. Zhuo, L., Hascall, V. C. & Kimata, K. Inter-alpha-trypsin inhibitor, a covalent protein-glycosaminoglycan-protein complex. *J. Biol. Chem.* **279**, 38079–82 (2004).

101. Choi-Miura, N.-H. *et al.* Purification and Characterization of a Novel Glycoprotein Which Has Significant Homology to Heavy Chains of Inter- -Trypsin Inhibitor Family from Human Plasma. *J. Biochem.* **117**, 400–407 (1995).

102. Lambin, P., Fine, J. M. & Steinbuch, M. Inhibition of plasmin by a small molecular weight inhibitor derived from human inter alpha trypsin inhibitor. *Thromb. Res.* **13**, 563–8 (1978).

103. Albani, D., Balduyck, M., Mizon, C. & Mizon, J. Inter-alpha-inhibitor as marker for neutrophil proteinase activity: an in vitro investigation. *J. Lab. Clin. Med.* **130**, 339–47 (1997).

104. Odum, L. Investigation of inter-alpha-trypsin inhibitor and slow migrating proteinase inhibitors in serum and urine. *Dan. Med. Bull.* **38**, 68–77 (1991).

105. Pratt, C. W. & Pizzo, S. V. In vivo metabolism of inter-α-trypsin inhibitor and its proteinase complexes: Evidence for proteinase transfer to α2-macroglobulin and α1-proteinase inhibitor. *Arch. Biochem. Biophys.* **248**, 587–596 (1986).

106. Kobayashi, H. *et al.* Inhibition of the soluble and the tumor cell receptor-bound plasmin by urinary trypsin inhibitor and subsequent effects on tumor cell invasion and metastasis. *Cancer Res.* **54**, 844–9 (1994).

Safety and disposal

Substance name, chemical formula	GHS-Symbol	Hazard Statements	Precautionary Statements	Disposal code*
Acetonitrile C_2H_3N		225, 332, 302, 312, 319	210, 240, 302+352+338, 403+233	1
Ammonium bicarbonate NH_4HCO_3		302	301+312+330	2
Dithiothreitol $C_4H_{10}O_2S_2$		302, 315, 319, 335	261, 302+352, 305+351+338	2
Formic acid CH_2O_2		226, 290, 302, 314, 331	P210, P280, P303+P361+P353, P304+P340+P310, P305+P351+P338, P403+P233	2
Iodoacetamide C_2H_4INO		301, 317, 334, 413	261, 280, 301+310, 342+311	2
Methanol CH_4O		225, 331, 311, 301, 370	210, 233, 280, 302+352, 304+340, 308+310, 403+235	1

*1: Disposal in the collecting tank for halogen-free, organic solvents and solutions.

*2: Disposal in the collecting tank for salt solutions, pH adjusted to 6-8.

Bio materials were disposed in the collecting bin for autoclave waste.

Acknowledgements

I would like to thank all people who supported me academically and personally to this point.

A special thank you goes my supervisor Prof. Dr. Hartmut Schlüter for welcoming me into his group in 2013 and having introduced me to the field of Proteomics. Thank you for your guidance and critically reviewing my work. Also, for trusting me with teaching and project management tasks.

I am thanking Prof. Dr. Sascha Rohn for agreeing to be my supervisor and reviewer. Also, for the tips and tricks regarding the bureaucracy of the University.

Within the group I had the honor of learning the quirks of mass spectrometry from Dr. Friedrich Buck and Dr. Marcel Kwiatkowski, thank you for letting me listen to your hour-long discussions.

I would like to thank Sönke Harder for all the technical support, thinking outside the box and coffee. Thank you, Dr. Marcus Wurlitzer for technical and emotional support and for all the interesting discussions. To Benjamin Dreyer, Dr. Christoph Krisp, Dennis Krösser and Dr. Lorena Wirt a special thanks for reviewing this thesis and keeping up the excellent mood in the lab, the office and after-hours.

Last but not least, I would like to thank my family and friends. My mother Sigi and my sister Lilli, for being my incredible Elsen, making me who I am and supporting me in every decision. Dieter Goetz and Ruben Figueiredo for the support and the encouragement in moving to Hamburg.

A special Thank you goes to Mareike Geidies, for your incredible support over the last year and for getting me to the finish line.

Thank you!

Acknowledgements

Eidesstattliche Versicherung (Affidavit)

Hiermit versichere ich an Eides statt, die vorliegende Dissertation selbst verfasst und keine anderen als die angegebenen Hilfsmittel benutzt zu haben. Die eingereichte schriftliche Fassung entspricht der auf dem elektronischen Speichermedium. Ich versichere, dass diese Dissertation nicht in einem früheren Promotionsverfahren eingereicht wurde.

Hamburg, 27. Juni 2019

Laura Heikaus